In vivo activity of B- and C-neurones in the paravertebral sympathetic ganglia of the bullfrog

Alexander Y. Ivanoff and Peter A. Smith*

Department of Pharmacology, University of Alberta, Edmonton, Alberta, Canada T6G 2H7

1. Spontaneous, *in vivo* synaptic activity was recorded from 146 B-cells and 60 C-cells in the IXth and Xth paravertebral sympathetic ganglia of the urethane-anaesthetized bullfrog. Sympathetic outflow to the blood vessels, which are innervated by C-cells, is different from that received by targets in the skin, which are innervated by B-cells.

2. B-cells were divided into three groups: the first (61 cells) exhibited only action potentials (APs) at 0·01–0·3 s^{-1}; the second (59 cells) exhibited APs and EPSPs and the third (26 cells) were silent. In addition to their usual suprathreshold input from the ipsilateral sympathetic chain, 53% of B-cells received subthreshold input which probably arose from fibres in the contralateral chain. 'Slow' B-cells exhibited less subthreshold activity and a slightly higher AP frequency than 'fast' B-cells. All B-cells are involved in a sympathetic reflex which is activated by tactile stimulation of the skin of the hindlimb. Activation of this reflex increased AP frequency without promoting long-lasting depolarization.

3. Sixty-seven per cent of C-cells exhibited rhythmic bursting activity with or without small intraburst EPSPs. Bursts tended to correlate with electrocardiographic (ECG) activity. The remainder exhibited an irregular pattern of activity which was not correlated with ECG activity and which included one to three APs and EPSPs interspersed between the bursts. Activity of both types of C-cell was inhibited following stimulation of the skin.

4. An average of twenty-three B-cells and twenty-one C-cells discharge simultaneously *in vivo*. This reflects branching of preganglionic fibres and results in synchrony of discharge in both postganglionic B- and C-fibres.

5. Stimulation of preganglionic C-fibres with five shocks at 20 Hz every 2 s to mimic C-cell bursting activity increased spontaneous activity in B-cells and in postganglionic B-fibres. *In vivo* activity in the C-fibre system may therefore modulate activity in B-cells via the ganglionic late–slow EPSP mechanism.

There are two major divisions of the peripheral sympathetic nervous system of amphibians; the B-fibre system and the C-fibre system (Nishi, Soeda & Koketsu, 1965; Honma, 1970; Dodd & Horn 1983*a*; Horn & Stofer, 1988; Smith, 1994). Peripheral targets for neurones in paravertebral sympathetic ganglia of the bullfrog (BFSG) include the bladder, mucous and granular glands, as well as blood vessels in the skin and in striated muscles. Stimulation of the preganglionic C-fibres causes vasoconstriction in the skin and muscle (Honma, 1970; Yoshimura, 1979; Horn, Fatherazi & Stofer, 1988; Stofer, Fatherazi & Horn, 1990), whereas stimulation of B-fibres produces secretion from cutaneous glands (Honma, 1970; Lang, Sjoberg & Skoglund, 1975), modulation of the sensitivity of cutaneous mechanoreceptors (Loewenstein, 1956) and a shortening of the recovery of arterioles which had been previously constricted following C-fibre stimulation (Yoshimura, 1979).

The B-fibre and C-fibre systems originate from separate groups of neurones in the spinal cord and remain anatomically separate as they pass through the paravertebral ganglia (Nishi & Koketsu, 1960; Dodd & Horn 1983*a*; Horn & Stofer, 1988; but see also Smith & Weight, 1986). Ganglionic B-cells are supplied by preganglionic B-fibres which emerge in the IVth, Vth and VIth roots, whereas preganglionic C-fibres supplying C-cells pass through the VIIth and VIIIth roots (Libet, Chichibu & Tosaka, 1968; Skok, 1973; Horn & Stofer, 1988). Stimulation of preganglionic fibres *in vitro* generates a fast nicotinic EPSP and a slow, muscarinic EPSP in B-cells (Tosaka, Chichibu & Libet, 1968; Weight & Votava, 1970),

* To whom correspondence should be addressed.

whereas C-cells exhibit a fast, nicotinic EPSP, a slow, muscarinic IPSP and a late–slow EPSP (Weight & Padjen, 1973*a*, *b*; Jan, Jan & Kuffler, 1979; Horn & Dodd, 1981; Dodd & Horn, 1983*b*). The late–slow EPSP is generated by the release of a peptide similar to luteinizing hormone-releasing hormone (Jan, Jan & Kuffler, 1980; Jones, Adams, Brownstein & Rivier, 1984). Peptide released following stimulation of C-fibres in VIIth or VIIIth spinal nerve is thought to diffuse within the ganglion so as to produce a late–slow EPSP in B-cells (Jan *et al.* 1979, 1980).

Although the cellular organization and biophysical properties of B- and C-neurones in the paravertebral sympathetic ganglia of various amphibians have been extensively investigated *in vitro* (Nishi *et al.* 1965; Skok, 1973; Ginsborg, 1976; Kuba & Koketsu, 1978; Adams, Jones, Pennefather, Brown, Koch & Lancaster, 1986; Smith, 1994), it is not known whether different types of peripheral target tissue receive specific patterns of activity from distinct subsets of ganglionic neurones, whether any integration of spinal sympathetic outflow occurs in ganglionic neurones or whether ganglionic peptides and non-nicotinic slow synaptic events have any role in ganglionic transmission *in vivo*. These questions have been addressed in the present study by exploiting the simplicity of organization of the discrete B- and C-fibre systems in the bullfrog and by making extracellular and intracellular recordings of their *in vivo* activity.

A preliminary report of some of this work has appeared (Ivanoff & Smith, 1993).

METHODS

Preparation

Bullfrogs (*Rana catesbeiana*) of either sex (weight 90–200 g) were anaesthetized with urethane (1·5–2·0 mg (g body weight)$^{-1}$) which was injected into the dorsal lymph sac. Although this single dose of anaesthetic was usually sufficient to immobilize the frogs for 6–8 h, provision was made for intravenous injection of supplementary doses of urethane (40 mg in 0·1 ml of Ringer solution) via a cannula placed in the femoral vein.

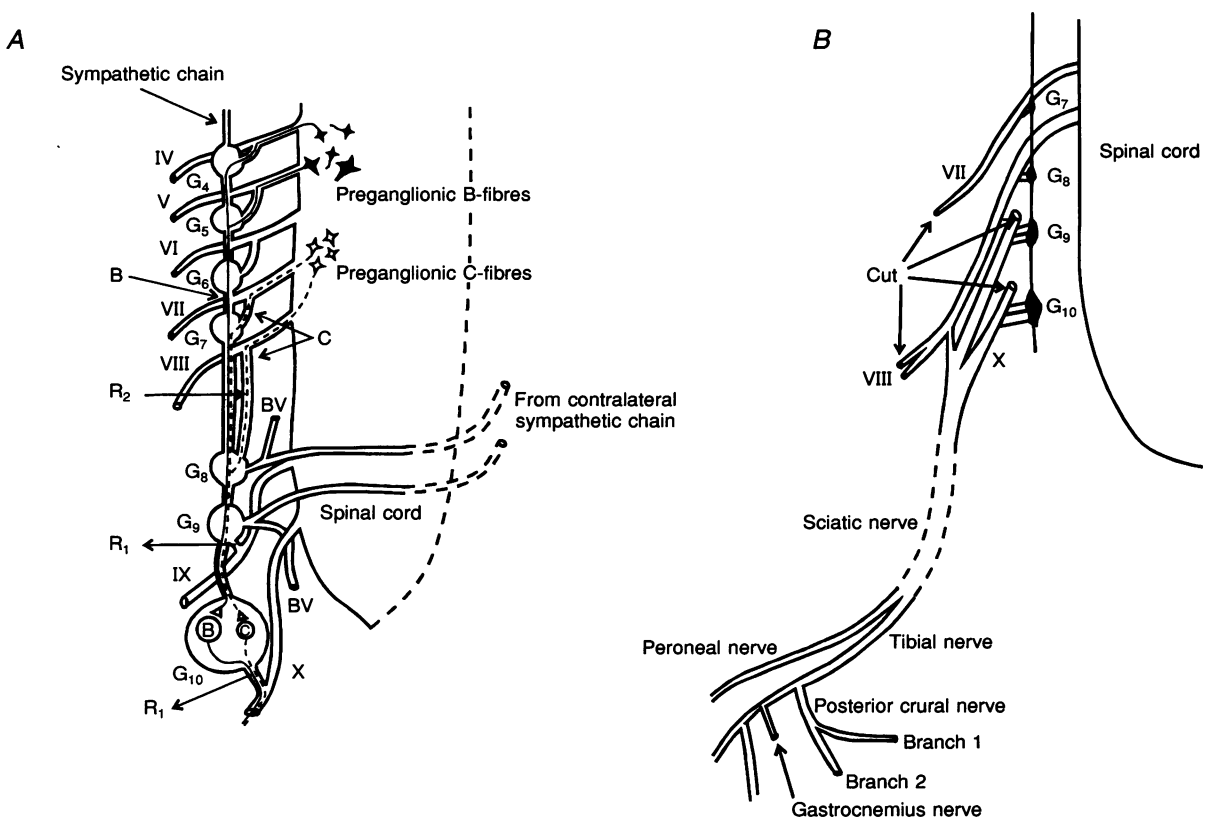

Figure 1. Diagrams to show anatomy and recording arrangements

A, schematic representation of bullfrog spinal cord and associated paravertebral sympathetic ganglia. Ganglia are labelled G_4 to G_{10} and their associated spinal nerves are labelled IV to X. The Xth ganglion is enlarged to allow schematic representation of B- and C-cells. R_1 and R_2 are recording points for extracellular suction electrodes (see text for details) and points B and C are points for cutting and stimulating preganglionic B- and C-fibres, respectively. Nerves labelled BV course towards blood vessels. *B*, diagram of recording points for peripheral sympathetic nerves. The connection of these nerves to the paravertebral ganglia and spinal cord is also illustrated to show how spinal nerves were cut to remove the influence of somatic nerves (see text for details).

Anaesthetized frogs were attached to a specially shaped plastic slab and positioned ventral side up. An incision was made in the left lower quadrant of the body cavity. Skin, underlying musculature and viscera were displaced and held in position by fine metal hooks attached to magnets which adhered to the steel surround of the plastic slab. The exposed area of the body cavity was superfused with frog Ringer solution which contained (mM): NaCl, 100; KCl, 2; $CaCl_2$, 1·8; Tris–HCl, 16 (pH 7·2); and D-glucose, 10. The IXth or Xth paravertebral sympathetic ganglion was positioned on a small (3 mm diameter) plastic base which was attached to a coarse micromanipulator. The ganglion was held in place by a small plastic ring attached to another coarse micromanipulator which was positioned so as to gently press it against the small plastic base. This constriction of the ganglion and surrounding tissue did not interrupt blood flow in the fine vessels which supply the ganglion because movement of blood cells within these vessels could be observed directly under the dissection microscope which was used to observe the preparation.

A high dose of urethane (up to 800 mg), which was sufficient to evoke cardiac arrest, was administered to each bullfrog at the end of the recording session. The animal was removed from the recording system and 'pithed' prior to disposal.

Intracellular and extracellular recording

Following careful removal of the connective tissue sheet between the ganglion and the plastic ring, ganglionic B- or C-neurones were penetrated with glass microelectrodes filled with 3 M KCl (resistance 60–120 MΩ). Voltage responses were recorded on one channel of a microelectrode amplifier (Axoprobe-1; Axon Instruments, Foster City, CA, USA). The other channel of this amplifier was used to monitor extracellular activity (AC coupled, filtered to −3 dB at 3 kHz). Spontaneous, population APs in one ramus communicantes, which contained postganglionic fibres from the IXth or Xth ganglion, was monitored with suction electrodes placed at recording point R_1 in Fig. 1*A*. In some experiments, the paravertebral sympathetic chain was cut and orthodromic activation of preganglionic B-fibres effected by placing the sympathetic chain in suction electrodes (point B in Fig. 1*A*). Preganglionic C-fibres were activated orthodromically by stimulation of the ramus communicantes which entered the VIIIth or occasionally the VIIth ganglion (point C in Fig. 1*A*). In other experiments, ganglionic neurones were activated antidromically by stimulation of the cut peripheral ends of the IXth or Xth spinal nerve. In preparations where preganglionic B-fibres were cut (at point B in Fig. 1*A*) to eliminate post-ganglionic B-fibre activity, postganglionic C-fibre activity was recorded from the rami which emerged from the IXth or Xth ganglia or from the fine nerves which run from these ganglia towards blood vessels (BV in Fig. 1*A*). In other experiments, suction electrodes were used to record from peripheral sympathetic nerves in the legs; the gastrocnemius nerve which supplies blood vessels in the gastrocnemius muscle and branches of the crural nerve (see Fig. 1*B*). In some experiments, the rami communicantes which enter the VIIth and/or VIIIth ganglion were cut (at point C in Fig. 1*A*) to eliminate C-fibre activity. All postganglionic activity recorded under these conditions was assumed to originate from B-fibres.

In preparations where *preganglionic* C-fibre activity was monitored, a few fibres in the VIIIth nerve ramus, which contains the C-fibres projecting to the IXth and Xth paravertebral ganglia, were drawn into a fine suction electrode which was prepared using an electrode puller which was intended for fabrication of patch-clamp pipettes. Because cutting one ramus and recording at point R_2 in Fig. 1*A* did not disrupt all C-fibre input to the IXth and Xth ganglia, it was possible to obtain pre- and postsynaptic recordings of C-fibre activity in the same animal (see Fig. 10*B*).

Bipolar electrocardiographic (ECG) recordings were made by inserting two steel needles under the skin. One was placed on the right side of the animal close to the heart and the other on the contralateral limb. Signals were AC coupled, amplified, filtered (to −3 dB at 100 Hz) and displayed on a rectilinear pen recorder (Gould 2400S, pen rise time < 8 ms). Intracellular and extracellular activity was usually monitored simultaneously and stored using a PCM data recorder (Vetter Instruments, Rebersburg, PA, USA) prior to analysis with pCLAMP software (Axon Instruments) on an IBM-type computer. Intracellular and extracellular activities were also recorded on a Nicolet type 2090 digital oscilloscope and/or on the pen recorder. The limited frequency response of the pen recorder attenuated the amplitude of intracellularly recorded APs by about 50% with little or no attenuation of their after-hyperpolarizations (AHPs). A Nicolet 4094 digital oscilloscope was used for signal averaging. In some experiments, intracellularly recorded APs were amplified and used to trigger the sweep for averaging (see Skok & Ivanoff, 1987; Ivanoff & Skok, 1992). Permanent records of the data from the Nicolet oscilloscopes were obtained from an X–Y plotter. Frequency histograms of spontaneous activity were created manually by measuring intervals between spikes or automatically by replaying data from the PCR recorder into a Labmaster TL-1 A/D converter attached to an IBM-type computer. Data were redigitized using the Fetchex software of the pCLAMP suite of programmes. The data were analysed using Fetchan and the histograms created using PStat. Wherever possible, numerical values are expressed as means ± S.E.M. and significance of difference is assessed using Student's unpaired, two-tailed t test.

RESULTS

Patterns of activity in identified B-cells

B-cells in the IXth or Xth paravertebral sympathetic ganglia were identified either by the conduction velocity of their axons following antidromic stimulation of spinal nerves or by the presence of spontaneous synaptic activity in preparations where preganglionic C-fibres in the rami communicantes between the VIIth and VIIIth and their respective paravertebral ganglia were cut. B-cells were additionally identified as those cells which exhibited orthodromic responses following stimulation of the paravertebral sympathetic chain between the VIth and VIIth ganglia. One hundred neurones were identified as B-cells after cutting the VIIth and VIIIth nerve rami and forty-six neurones were identified by antidromic stimulation. There was no obvious difference in the patterns of activity of cells identified by the different methods.

Synaptic activity was evident in 120 of these 146 cells. The resting membrane potential (E_m) varied from −43 to −70 mV (average value −55·8 ± 1·2 mV, $n = 41$). B-cells were divided into three groups on the basis of their pattern of activity. Variations in B-cell activity pattern were not a consequence of different levels of urethane anaesthesia in different experiments because examples of all three types of activity were encountered in every animal tested. The first

group of B-cells (61 of out of 146) exhibited only APs that usually appeared sharply without any apparent inflexion on the rising phase. Recordings from a cell of this type are illustrated in Fig. 2*A a*. There was considerable variation in the frequency of APs in this group (from 0·01 to 0·3 s^{-1}).

The second group of cells (59 out of 146) exhibited synaptic activity which included EPSPs which in some, but not in all cells exceeded threshold for AP generation. This type of activity is illustrated in Fig. 2*A b*. Although the frequency of events (APs and/or EPSPs), which ranged from 0·06 to

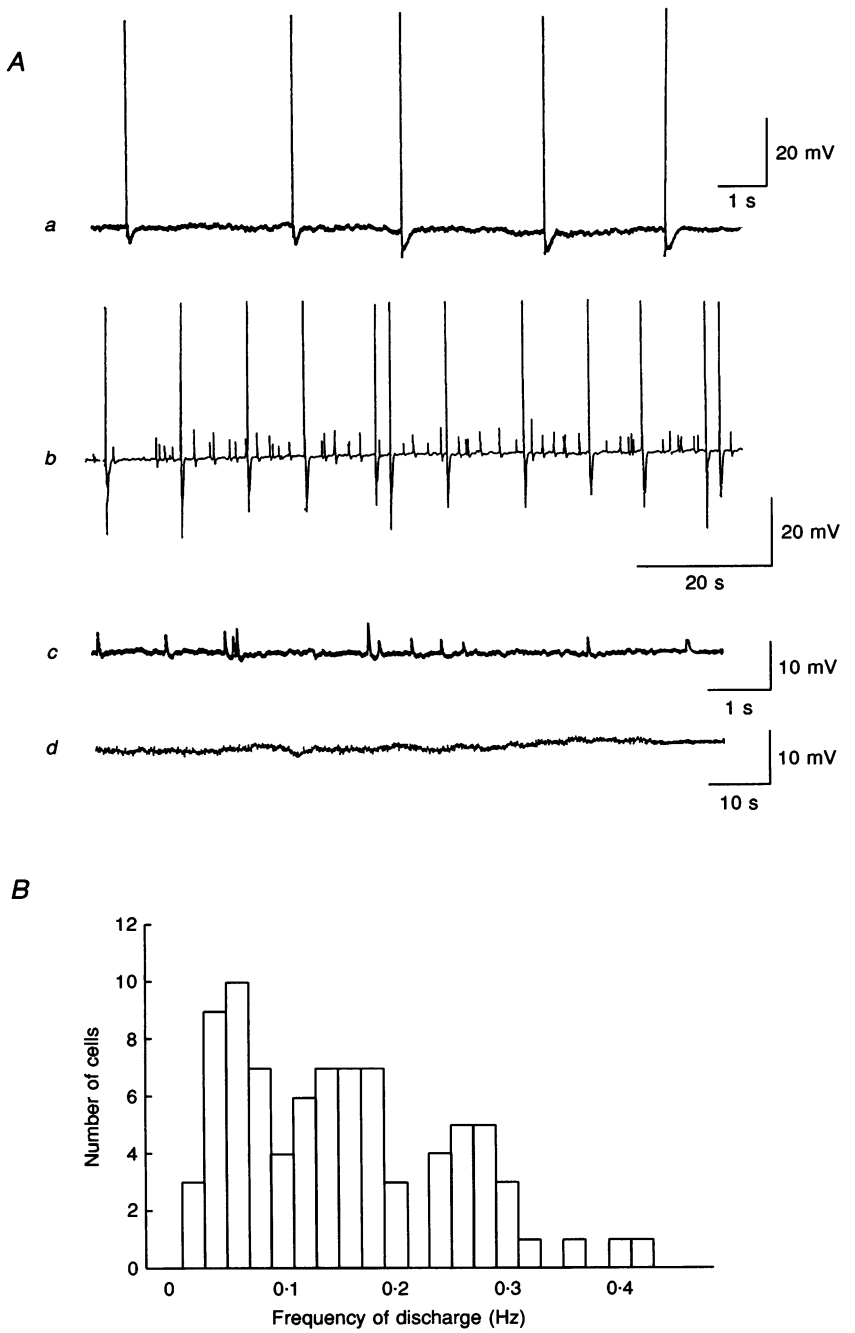

Figure 2. B-cell activity *in vivo*

A, intracellular microelectrode recordings of different types of activity in identified B-cells; *a*, cell exhibiting APs only; *b*, cell exhibiting APs and subthreshold EPSPs; *c*, cell exhibiting subthreshold EPSPs only; *d*, silent cell. Data records in *b* and *d* from rectilinear pen recorder. Note that the spike amplitude is limited by the limited frequency response of the pen. Records in *a* and *c* from data collected and stored on videotape, redigitized using pCLAMP software, stored in computer and replotted on an *X–Y* plotter. *B*, histogram to show distribution of frequencies of AP discharge for 111 B-cells.

$0{\cdot}4\ s^{-1}$, was more rapid than in the first group of cells, there was no significant difference in the mean frequencies of APs between the two groups ($0{\cdot}21 \pm 0{\cdot}04\ s^{-1}$, $n = 61$ and $0{\cdot}25 \pm 0{\cdot}03\ s^{-1}$, $n = 50$; $P > 0{\cdot}4$). Usually, the frequency of EPSPs was similar to or slightly higher than the frequency of APs in any given cell. This second group of B-cells could be subdivided into three further subgroups: nine out of fifty-nine cells exhibited only subthreshold EPSPs (see Fig. 2*A c*) yet would exhibit robust APs in response to injection of depolarizing current via the microelectrode; twenty-three out of fifty-nine cells exhibited APs and EPSPs of constant amplitude; and twenty-seven out of fifty-nine cells exhibited APs and EPSPs of varying amplitudes.

The histogram shown in Fig. 2*B* summarizes the broad variation in discharge rates for the 111 B-cells which exhibited spontaneous APs.

The third group of B-cells (26 out of the 146 cells) were silent (Fig. 2*A d*) and exhibited no synaptic activity during the period of recording (in most cases more than 10 min). These cells did, however, generate an AP in response to direct stimulation through the microelectrode.

Since intracellular recording provides no information about the total ganglionic B-fibre outflow, recordings were made from the rami communicantes of the IXth or Xth ganglion (point R_1 in Fig. 1*A*) after the preganglionic C-fibre input had been cut. It was our impression that rami from the IXth ganglion contained more B-fibres than those from the Xth ganglion. The typical recordings illustrated in Fig. 3 show that a 3–7 s silent period appears after a strong discharge. The variation in amplitude of the discharge reflects variations in the number of synchronously discharging B-fibres contributing to each event. Discharge of any single B-cell is therefore likely to be correlated with the discharge of several other B-fibres (see Figs 5*A* and 6*B*). The upper record in Fig. 3 is an ECG recording and the lower records were obtained from postganglionic B-fibres. There is no synchronization of B-fibre activity and the ECG. The vast majority of the neuronal activity that is illustrated in Fig. 3 originates from B-cells because it was almost completely eliminated when the paravertebral sympathetic chain was cut between the VIth and VIIth ganglia (Fig. 3*Bc*). The infrequent, low-amplitude responses that remain were eliminated when the fine nerves which run to the ganglia

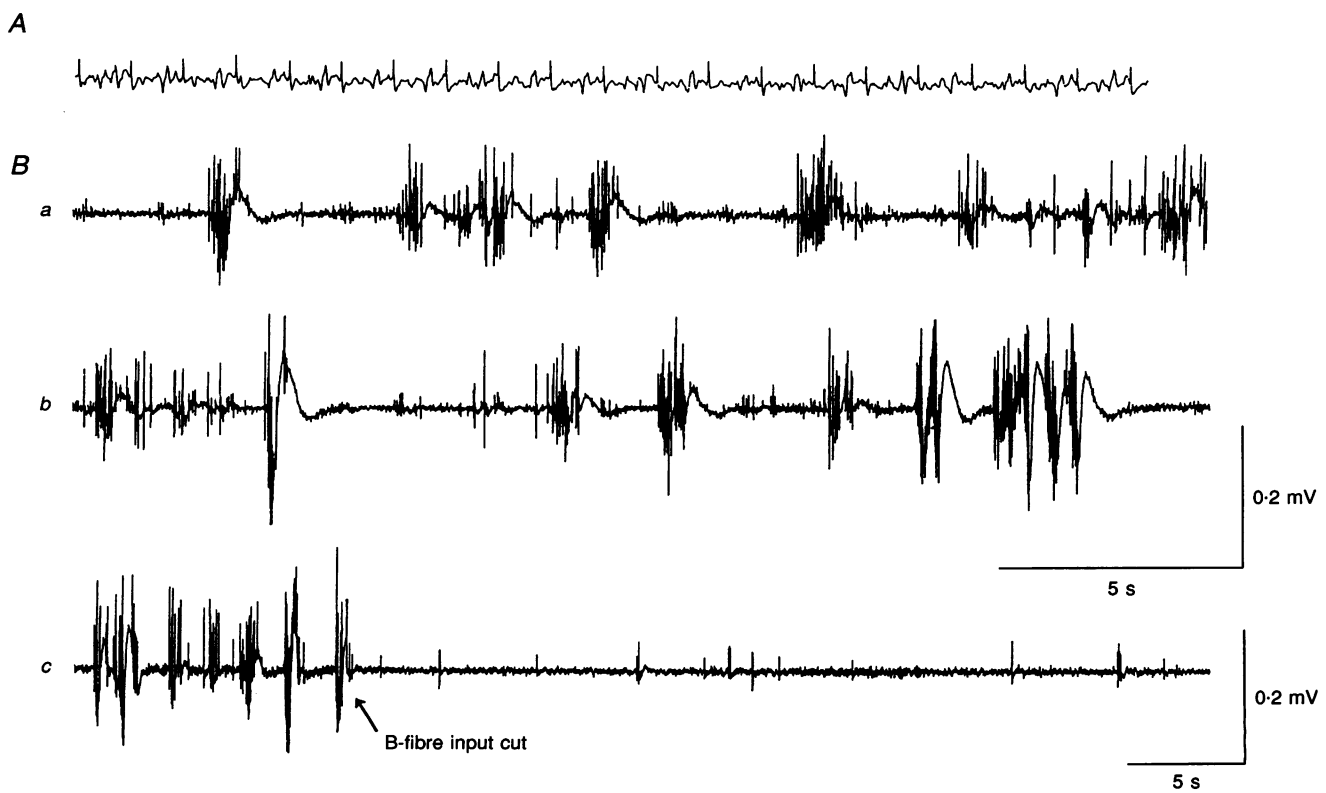

Figure 3. Postganglionic B-fibre activity *in vivo*

Extracellular suction electrode recordings from a ramus which emerged from the Xth ganglion are compared with ECG activity. Since the C-fibre input was interrupted by cutting the VIIth and VIIIth nerve rami, the recordings illustrated originate almost entirely from B-fibre activity. *A*, ECG recordings. *Ba–c*, continuous record of B-fibre activity which was greatly reduced but not abolished when the paravertebral sympathetic chain was cut between the VIIth and VIIIth ganglia. Recordings from rectilinear pen recorder. Note slow time scale applies to record *c* only. Calibration for ECG records is the same as for recordings of nerve activity.

from beyond the mid-line of the animal were cut (data not shown). This suggests that the infrequent, low-amplitude activity may have originated from the contralateral sympathetic chain (see Fig. 1*A*).

In 107 out of the 111 B-cells, which exhibited spontaneous APs, the response exhibited a sharp rising phase, suggesting it had been generated by a rapidly rising EPSP as would be produced by a single presynaptic B-fibre (Fig. 4*A*; Nishi & Koketsu, 1960; Nishi *et al.* 1965; Weitsen & Weight, 1977; Smith & Weight, 1986). In the remaining four cells, however, there was an obvious fluctuation in the rate of rise of successive EPSPs. A recording from one such cell is illustrated in Fig. 4*B*. These cells, as well as the fifty-nine cells which exhibited subthreshold EPSPs, may receive a convergence of synaptic input (see Discussion).

There was considerable variation in the shape of the AHP in 22 of the 111 B-cells which exhibited spontaneous APs. For example, the AHPs in the data record presented in Fig. 2*A b* vary from 7 to 12 mV in amplitude and there is considerable variation in AHP amplitude in the cell illustrated in Fig. 4*B*. This may reflect variations in the temporal relationship between the onset of the EPSP and the generation of the AP and 'short circuiting' of the K^+ currents that generate the AHP by the decrease in membrane resistance which accompanies the EPSP.

Dodd & Horn (1983*a*) divided the B-cell population into two subgroups; 'fast' and 'slow' B-cells were defined as those cells with antidromic conduction velocities that were greater than, or less than 1 m s^{-1}, respectively. Based on this criterion, all antidromically tested cells in the present experiments with antidromic conduction velocities from 0·4 to 2·5 m s^{-1} were divided into two groups; 'fast' B-cells (29 neurones) and 'slow' B-cells (17 neurones). The average antidromic conduction velocity of fast B-cells was $1{\cdot}85 \pm 0{\cdot}06$ m s^{-1} ($n = 29$) and $0{\cdot}65 \pm 0{\cdot}07$ m s^{-1} for slow B-cells ($n = 17$). The average frequency of APs in slow B-cells ($0{\cdot}22 \pm 0{\cdot}03$ s^{-1}, $n = 17$) was higher than that in fast B-cells ($0{\cdot}14 \pm 0{\cdot}03$ s^{-1}, $n = 2$; $P < 0{\cdot}001$) and although both cell types exhibited the three B-cell activity patterns described above, subthreshold EPSPs occurred more frequently in 'fast' B-cells; 57% of 'fast' B-cells exhibited subthreshold EPSPs with or without APs, 18% exhibited APs only and 25% were silent. By contrast, 28% of 'slow' B-cells exhibited both APs and subthreshold EPSPs, 50% exhibited APs only and 22% were silent.

In four B-cells from four different animals, slow, spontaneous depolarizations of the membrane were observed. These events were not obviously associated with movement artifacts resulting from skeletal muscle contraction or from changes in blood flow which could provoke movement of blood vessels close to the ganglia. Slow depolarizations were usually associated with a discharge of APs that appeared synchronously with spontaneous bursts of activity in the postganglionic fibres. Some typical events are illustrated in Fig. 5*A*. The upper traces are intracellular microelectrode recordings and the lower records are extracellular (suction electrode) recordings from the postganglionic axons in the ramus communicantes (point R_1 in Fig. 1). The amplitude and duration of the slow depolarization ranged from 3 to 7 mV and from 20 to 60 s. Preganglionic B-fibre and C-fibre inputs were left intact in all preparations which exhibited these responses.

Activation of B-cells by stimulation of the skin

Honma (1970) and Horn *et al.* (1988) showed that B-cells innervate targets in the skin. Since targets of sympathetic nerves often give rise to sensory fibres which participate in reflex activation of the sympathetic system (Janig, 1988; Janig & McLachlan, 1992), we tested whether a reflex response could be evoked in B-cells following tactile stimulation of the skin of the hindlimb. Immediately after

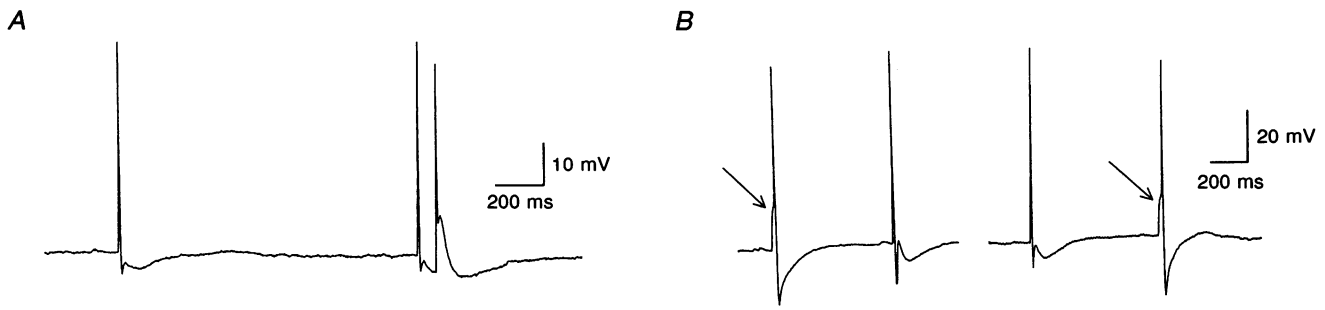

Figure 4. Variation in the rising phase of the AP and its AHP during intracellular recording from B-cells

A, recordings from a 'typical' B-cell which exhibited APs with a steep rising phase. *B*, recordings from 1 of 4 B-cells in which the AP exhibited a 'hump' in the rising phase (indicated by arrow) because the AP sometimes arose after the initial, slow rising phase of the EPSP. Note variation in AHP amplitude in this cell. Data originally stored on videotape, redigitized using pCLAMP software, stored in computer and replotted on an *X–Y* plotter.

touching the skin with a blunt metal probe, all ('fast' and 'slow') B-cells generated one or a few APs. Mild nociceptive stimulation (forceps pinch) produced responses in B-cells which were indistinguishable from those evoked by simply touching the skin. The response illustrated in Fig. 6*A* is typical in that skin stimulation evoked a brief, transient discharge of APs prior to prompt re-establishment of the original discharge rate. In a few cells, including some 'silent' B-cells, the frequency of APs was increased for 2–3 min following the stimulation (Fig. 6*B*). This part of

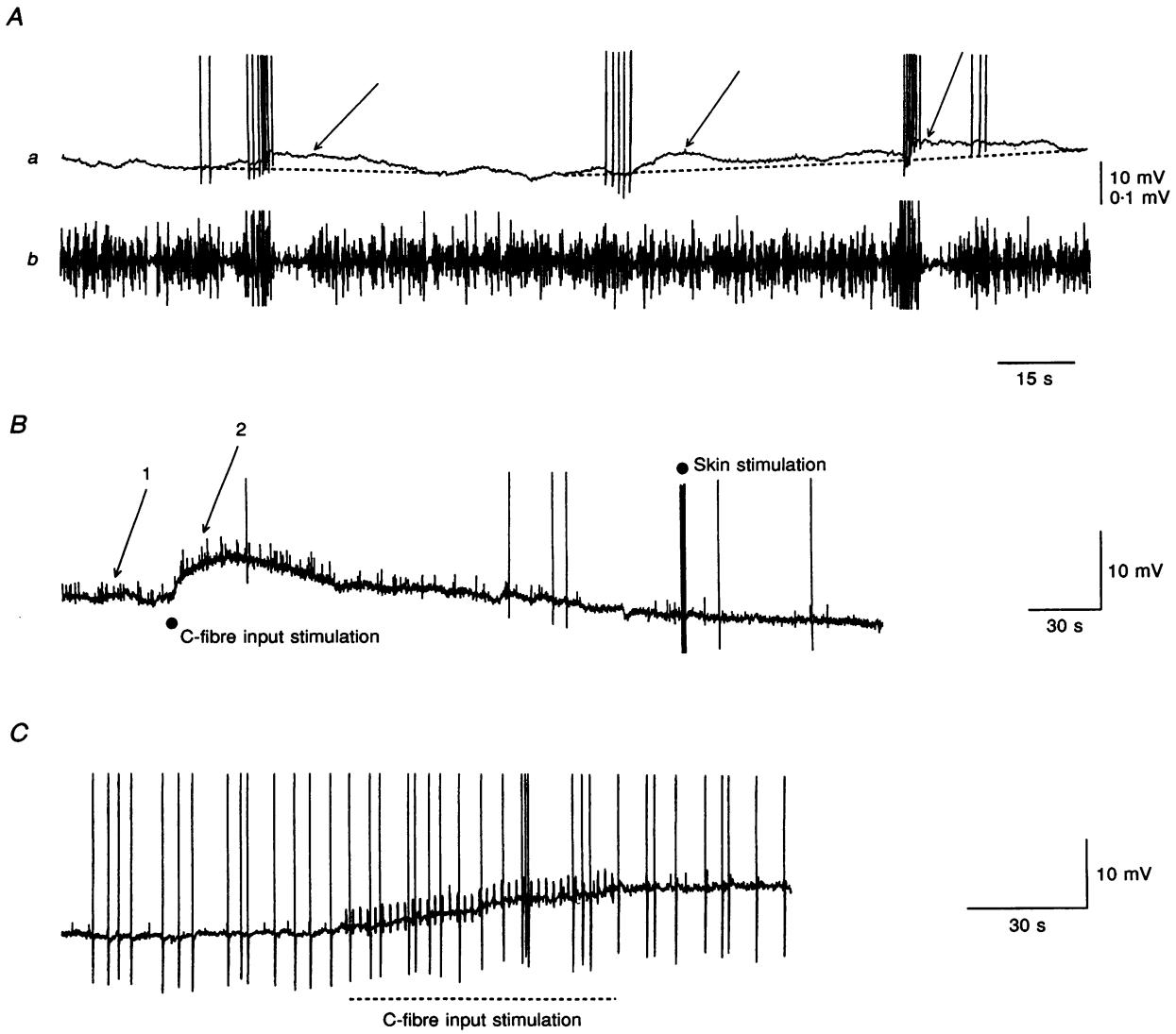

Figure 5. Slow depolarizations in B-cells

A, spontaneous events (indicated by arrows) associated with discharge of APs. Trace *a*, intracellular microelectrode recording; trace *b*, simultaneous extracellular recording from postganglionic ramus communicans. Note that bursts of activity recorded intracellularly are correlated with bursts of population activity in the postganglionic nerve. *B*, effects of tetanic C-fibre stimulation (30 Hz; 5 s) and skin stimulation on E_m and activity in another B-cell. The slow depolarization is a late–slow EPSP Note that although spontaneous, fast EPSPs which occur during the late–slow EPSP (small upward deflections designated by arrow 2) are larger than those which occur prior to the response (marked by arrow 1), there is no obvious increase the frequency of spontaneous APs. *C*, effect of 'physiological' or 'burst' stimulation of preganglionic C-fibres (5 shocks at 20 Hz once every 2 s; the small, regular deflections observed during the stimulus period are stimulus artifacts; stimulus period is designated by a dashed line). Note slight increase in B-cell AP frequency following stimulation. Recordings from rectilinear pen recorder, spike amplitudes (intracellular and extracellular) are limited by the frequency response and excursion of the pen). 10 mV calibrations refer to intracellular recordings and 0·1 mV calibration refers to extracellular recordings. The 15 s calibration refers to both records in *A*. Preganglionic C-fibres were left intact in the preparation illustrated in *A* but were cut in the preparations illustrated in *B* and *C*.

the figure also shows that activity evoked in single B-cells by skin stimulation was synchronized with discharges in the postganglionic fibres. Since postganglionic B-fibres had to be cut to obtain these extracellular recordings, the activity evoked in B-cells as a result of skin stimulation is not a consequence of antidromic activation of B-fibre terminals.

Slow changes in E_m did not usually occur during or after tactile or nociceptive stimulation of the skin. In the few cells in which slow depolarizations were observed, such responses were not repeatable. By contrast, discharges of APs in B-cells were evoked with high reproducibility following skin stimulation. The consistency of this response was established during the course of our study and as experiments progressed, it was used as an additional criterion to confirm the identification of B-cells.

In preparations where the preganglionic C-fibres were cut, these fibres were activated with a single stimulus to the ramus communicans which entered the VIIth or VIIIth ganglion. These experiments tested whether C-fibres converge onto presumed B-cells, which continue to exhibit spontaneous synaptic activity as a result of their B-fibre input. No response was observed in any of forty-seven B-cells tested (see Nishi & Koketsu, 1960; Dodd & Horn, 1983*a*).

Late–slow EPSP in B-cells *in vivo*

By contrast with the lack of effect of a single stimulus, tetanic stimulation of preganglionic C-fibres (30 Hz, 5 s) evoked a late–slow EPSP in all five B-cells tested. This response results from diffusion of LHRH from C-fibre terminals (Jan *et al.* 1979, 1980). In B-cells which exhibited spontaneous subthreshold nicotinic EPSPs, the late–slow EPSP increased their amplitude but in no case was a transition from subthreshold to suprathreshold activity demonstrated (see Schulman & Weight, 1976). Activation of the late–slow EPSP mechanism also did not seem to promote generation of spontaneous APs as a result of alteration of the properties of ion channels in the B-cell membrane (see Dodd & Horn 1983*b*; Jones, 1985). Stimulation of the VIIth connecting ramus was more consistent in producing a late–slow EPSP than stimulation of the VIIIth ramus. In the experiment illustrated in Fig. 5*B*, a single tetanic stimulus to preganglionic C-fibres produced a late–slow EPSP in a B-cell. The cell was identified by its response to stimulation of the skin. This response was typical in that the amplitude of subthreshold spontaneous nicotinic EPSPs was increased yet there was no obvious increase in the frequency of spontaneous APs.

These data confirm that the E_m of B-cells can be modulated through the activation of preganglionic C-fibres (Jan *et al.*

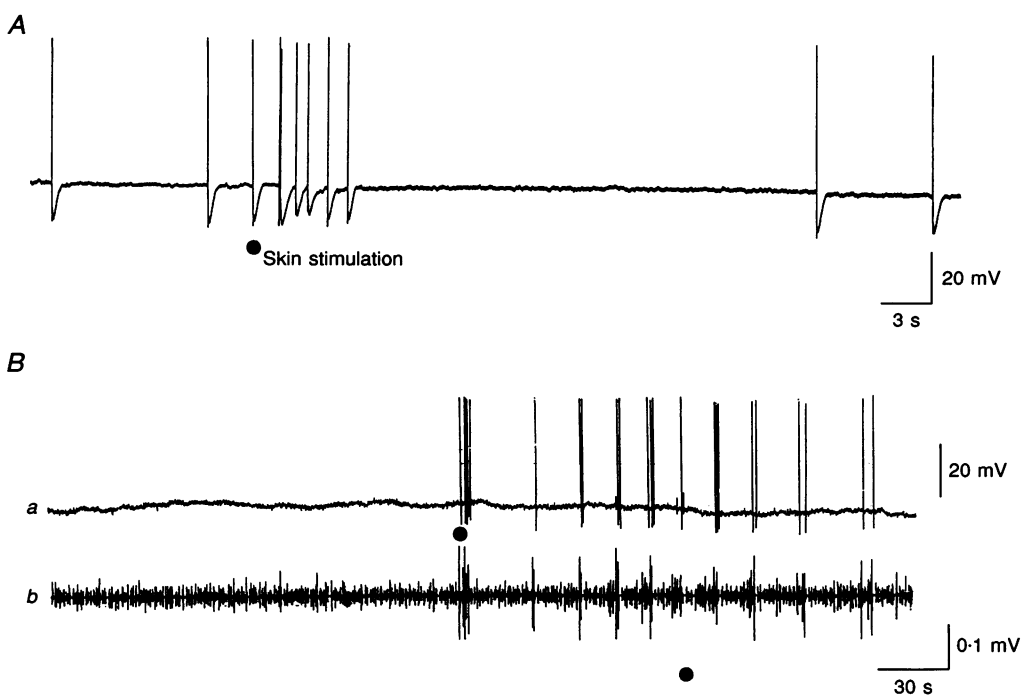

Figure 6. Effects of skin stimulation on spontaneous activity in two different B-cells

A, typical response which involves transient burst of APs and prompt resumption of normal discharge rate. *B*, less typical response in a 'silent' B-cell in which skin stimulation produced a lasting increase in discharge rate for several minutes: *a*, intracellular recording; *b*, extracellular recording of population activity in postganglionic ramus communicans. Note correlation between extracellular activity and activity seen in single B-cell. Trace in *A* was an intracellular recording stored on videotape and output on *X–Y* plotter as described in legend to Fig. 2. Traces in *B* were from rectilinear pen recorder (spike amplitudes attenuated by the limited frequency response of the pen).

1979; 1980). To examine whether this modulation might occur *in vivo*, intracellular recordings were made from B-cells in preparations where preganglionic C-fibres were cut and the VIIth or VIIIth nerve rami were drawn into stimulating electrodes. To mimic the bursting activity which is characteristic of C-fibres *in vivo* (see below), either ramus was stimulated once every 2 s with five shocks at 20 Hz. This type of stimulation produced a 3–7 mV depolarization in six out of nine cells tested. This response was slower but similar to that produced by a single tetanic stimulus (Fig. 5*B*). Unlike a single tetanus, however, repeated brief bursts of stimuli slightly, yet significantly, enhanced spontaneous activity in all cells tested. In the experiment illustrated in Fig. 5*C*, the AP frequency prior to stimulation was 0·2 Hz and this increased to 0·26 Hz after stimulation. Mean AP frequency increased from $0{\cdot}16 \pm 0{\cdot}02$ to $0{\cdot}21 \pm 0{\cdot}05$ Hz following stimulation ($n = 9$; $P < 0{\cdot}05$).

In other experiments, extracellular recordings of B-fibre activity were made from a postganglionic nerve ramus in preparations where preganglionic C-fibres were cut and stimulated once every 2 s with five shocks at 20 Hz. As shown in Fig. 7, this 'burst' stimulation enhanced spontaneous B-fibre activity during the stimulation period and evoked a lasting after-discharge which was reflected as increased noise in the recording after the stimulation had ceased. This effect was observed in all seven preparations tested. It would therefore appear that *in vivo* cross-talk might occur between the C- and B-fibre systems at the level of the ganglion.

Patterns of activity in identified C-cells

Neurones which satisfied any of the following criteria were identified as C-cells. (i) C-cells continued to exhibit spontaneous synaptic activity in preparations in which B-fibre input was interrupted by cutting the paravertebral sympathetic chain between the VIth & VIIth ganglion;

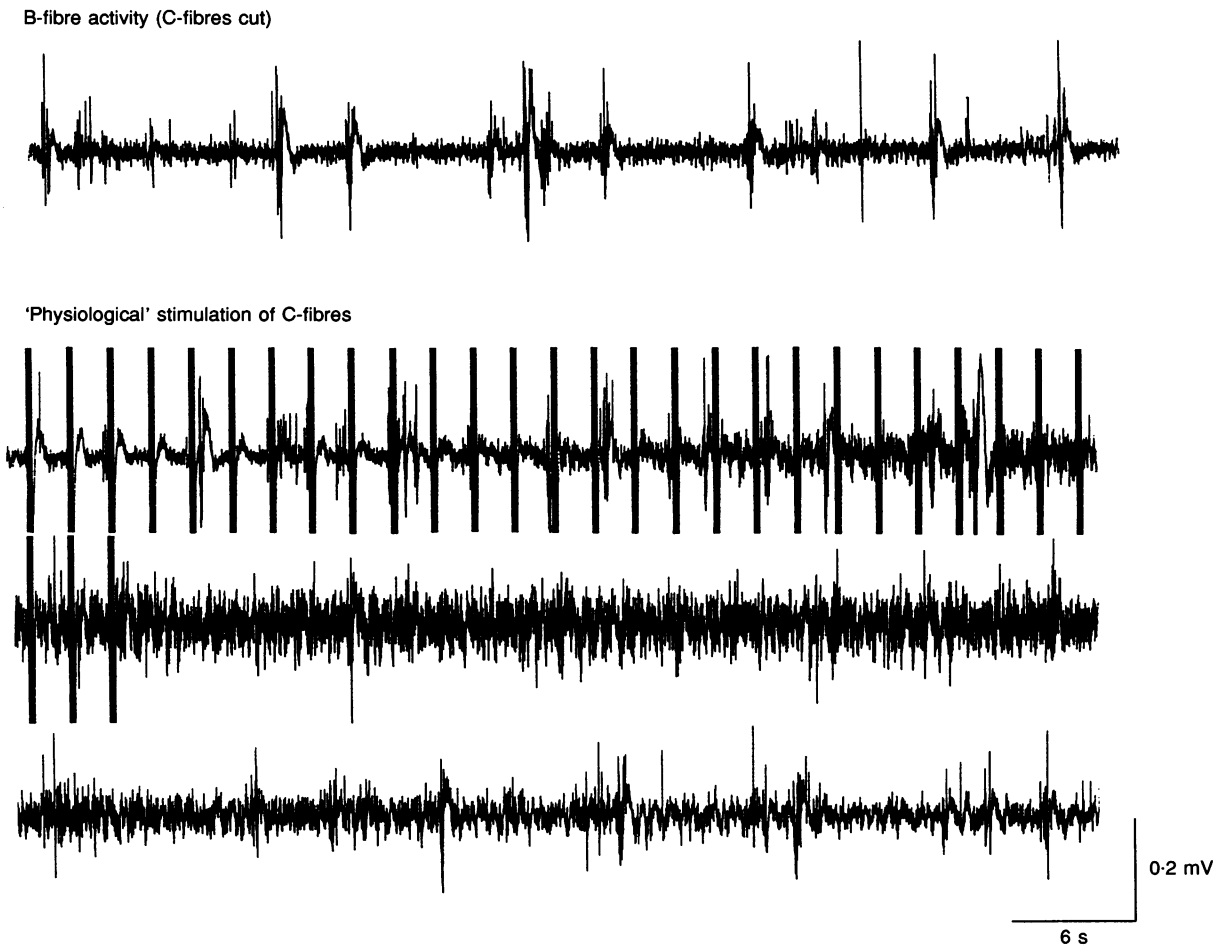

Figure 7. Interaction between B- and C-fibres in BFSG *in vivo*

Extracellular recording of B-fibre activity in a postganglionic ramus from a Xth ganglion in which the C-fibre input had been interrupted by cutting the VIIth and VIIIth nerve rami. Effect of 'physiological' stimulation of preganglionic C-fibres (5 shocks at 20 Hz once every 2 s; large, regular deflections are stimulus artifacts). Note increase in B-fibre activity produced during stimulation period and increased noise (indicative of increased discharge) which persists after stimulation is ceased. Continuous record from rectilinear pen recorder.

(ii) C-cells exhibited an axonal conduction velocity $< 0{\cdot}4$ m s^{-1} following antidromic stimulation of spinal nerves; (iii) C-cells exhibited orthodromic responses following stimulation of the rami communicantes which enter the VIIth or VIIIth ganglion (see Fig. 1*A*).

Successful intracellular penetration was achieved in sixty C-cells. The E_m varied from −38 to −60 mV (mean value $-41{\cdot}6 \pm 1{\cdot}2$ mV, $n = 26$). Two-thirds of the cells (67%), such as that illustrated in Fig. 8*A*, exhibited bursts of synaptic activity with or without interburst EPSPs. The remainder exhibited a more complex and irregular pattern of activity which included single APs interspersed between short bursts of APs as well as EPSPs of different amplitudes. Recordings from a cell which exhibited this type of activity are shown in Fig. 8*B* and *C*. Unlike B-cells, where 18% of the population were silent (Figs 2*A d* and 6*B*), all C-cells exhibited some form of spontaneous activity. All C-cells

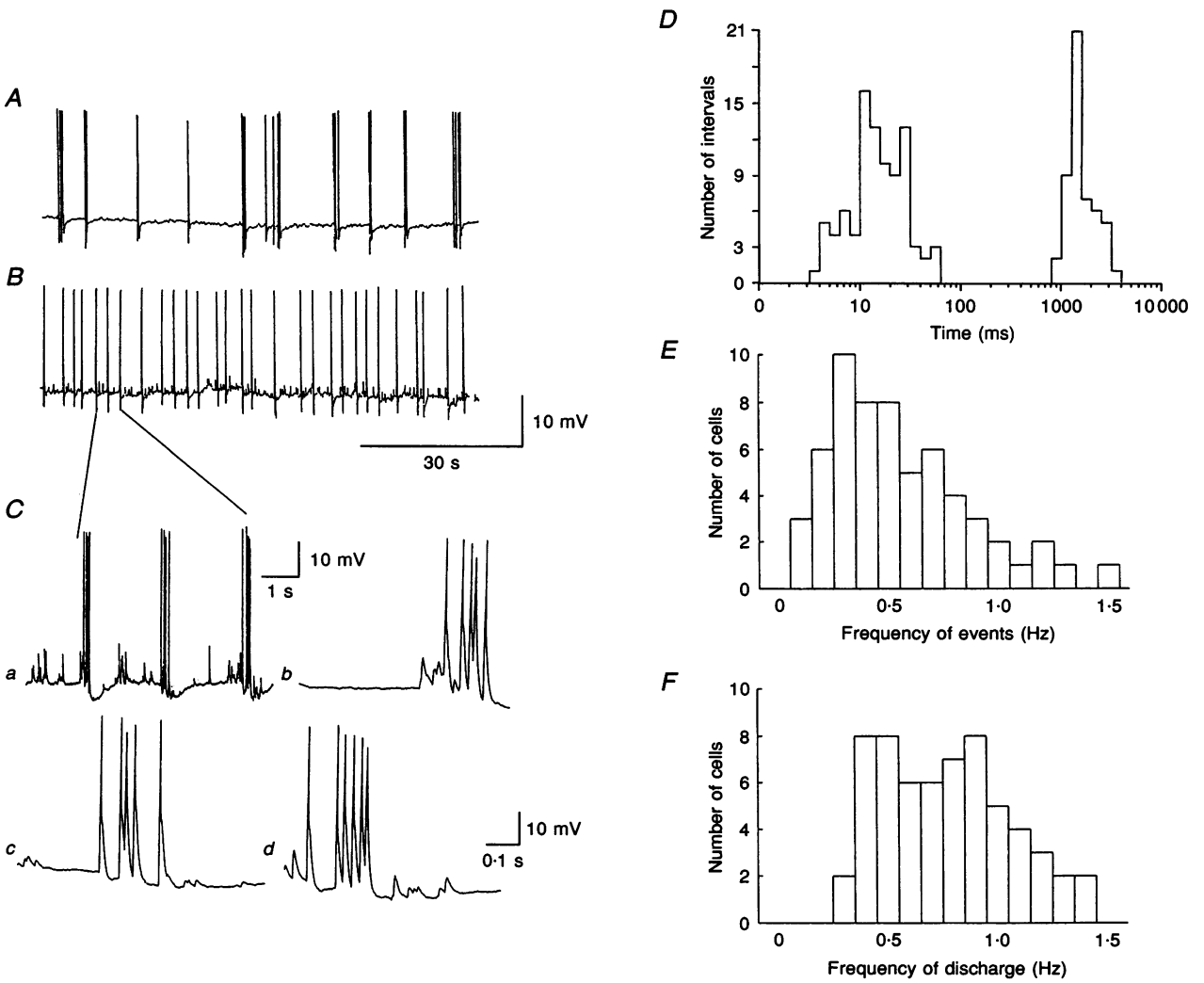

Figure 8. Spontaneous synaptic activity recorded intracellularly in C-cells

A, recordings from a typical cell exhibiting bursts of activity. *B*, recordings from another cell which exhibited bursts of activity interspersed with subthreshold EPSPs. At the slow chart speed, bursts of 6 APs show as single, large deflections. *C*, when activity from the cell shown in *B* is shown on faster time scales, bursts containing as many as 6 APs are clearly visible. The 1 s calibration refers to record *a* and the 0·1 s calibration refers to records *b*, *c* and *d*. *D*, interval histogram for APs occurring in the cell illustrated in *B* and *C*. Data acquired from 50 s of recording which was digitized and analysed using pCLAMP (Fetchex, Fetchan and PStat) software. *E*, frequency histogram for 60 C-cells; in this analysis each burst of APs and each single AP was considered to be an 'event'. *F*, alternative frequency histogram for the same 60 cells; in this analysis, the average number of single and/or intraburst APs occurring in each cell per 1 s is measured and the discharge frequency calculated to yield the total number of spikes over a 1 s time period. Frequencies of events in each cell are allocated to the appropriate 0·1 Hz bin to produce the histograms in *E* and *F*. Records in *C* were originally stored on videotape and output on an *X*–*Y* plotter. Data records in *A* and *B* from rectilinear pen recorder (spike amplitudes limited by limited frequency response or maximum excursion of the pen).

that were unequivocally identified by the conduction velocity of their axons exhibited spontaneous burst activity (the range of conduction velocities of these cells was from 0·16 to 0·38 m s^{-1}; the mean was 0·23 ± 0·01 m s^{-1}; $n = 10$). The bursts lasted from 0·1 to 0·5 s and usually comprised four to six APs. As shown in Fig. 8*C*, most C-cell APs arose sharply from an EPSP with no obvious inflexion in the rising phase. Occasionally, however, APs occurred later during the rising phase of the EPSP.

The similarity between the frequency of APs within the bursts and the frequency of spontaneous subthreshold EPSPs suggests that the burst activity results from the activity of preganglionic fibres rather than from the intrinsic biophysical properties of the C-cells (see Horn & Dodd, 1983*b*). An interval histogram for AP discharge in the C-cell illustrated in Figs 8*B* and *C* is shown in Fig. 8*D*. The distribution is bimodal, reflecting the interburst interval and the much shorter intervals between APs within the burst.

The average frequency of occurrence of bursts of APs was 0·56 ± 0·04 s^{-1} ($n = 60$). The average frequency of occurrence of all APs (i.e. interburst APs and bursts comprising several APs) ranged from 0·35 to 1·6 s^{-1} (mean 0·7 ± 0·04 s^{-1}). Although the frequency of APs within the bursts is > 10 Hz, the bursts occur infrequently so that the total number of APs per second is very much lower than the frequency within the burst. Figures 8*E* and *F* show two different summaries of spontaneous synaptic activity in the sixty C-cells which were studied. In Fig. 8*E*, each burst or single AP is considered as an 'event' and the regularity of occurrence of different mean frequencies is presented. Figure 8*F* illustrates the average number of single and/or intraburst APs occurring within 1 s.

Smith & Weight (1986) described a small population of C-cells which received input from B-fibres in addition to their normal input from preganglionic C-fibres. Single or repetitive electrical stimulation of the paravertebral sympathetic chain, which contains B-preganglionic fibres, did not, however, evoke any synaptic response in any of the 15 C-cells which were tested *in vivo*.

Inhibition of C-cells by stimulation of the skin

Afferent stimuli applied to the skin of the hindlimb (a touch or a pinch) which consistently evoked excitatory responses in B-cells, weakly but consistently inhibited spontaneous synaptic activity in C-cells. Inhibition of activity in three different C-cells, which exhibited different

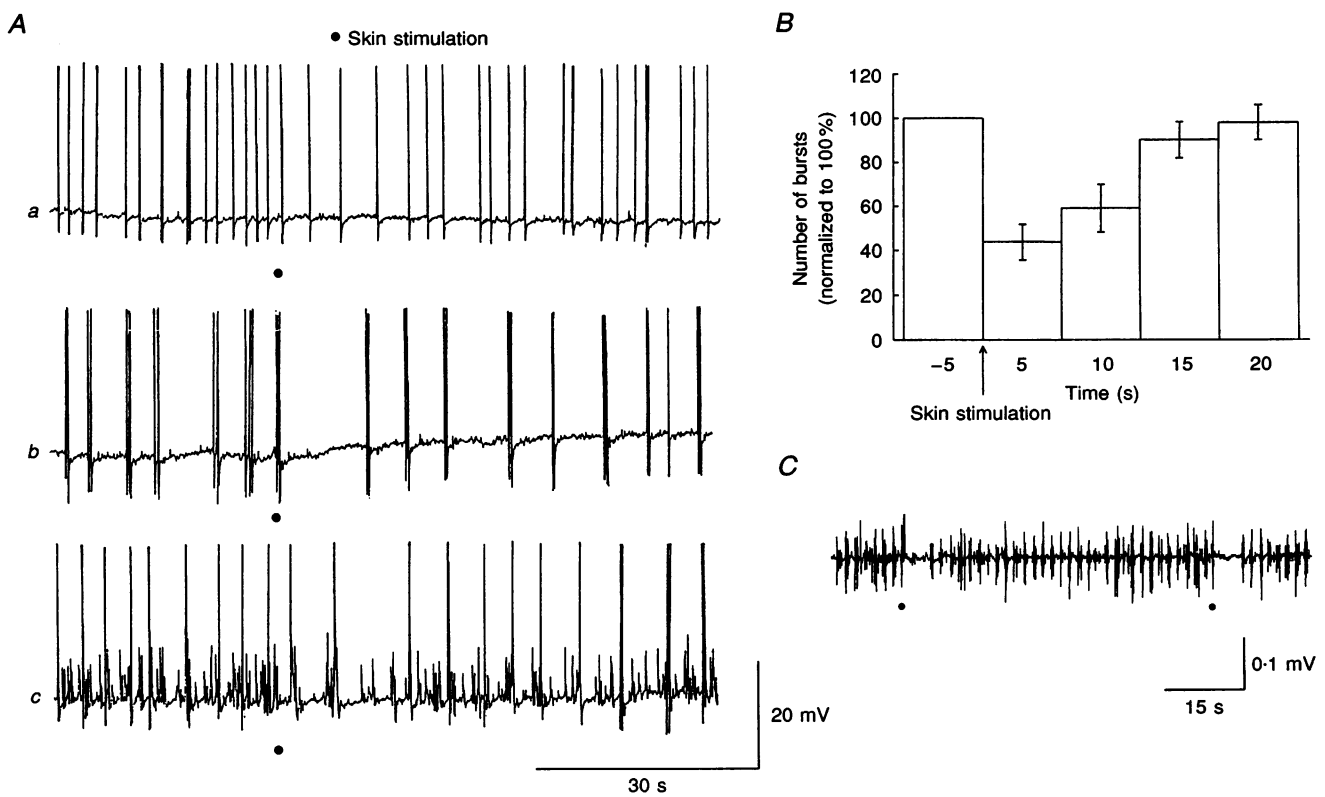

Figure 9. Effects of skin stimulation on spontaneous synaptic activity in C-cells

A, intracellular recordings from three different cells. *B*, peristimulus histogram showing decrease in occurrence of bursts in 6 C-cells following stimulation of the skin (see text for details). *C*, effects of skin stimulation on C-fibre activity recorded from a postganglionic ramus communicans in a preparation where descending B-fibre input was cut. Note depression of spontaneous intracellular activity and population C-fibre activity. Records from rectilinear pen recorder (spike amplitudes limited by maximum available excursion of the pen and/or by its limited frequency response).

patterns of spontaneous activity is illustrated in Fig. 9*A*. Inhibition of C-cell activity is more clearly demonstrated by the effect on extracellularly recorded C-fibre activity in the Xth nerve ramus in a preparation in which preganglionic B-fibres had been cut (Fig. 9*C*) and by the peristimulus histogram shown in Fig. 9*B*. Data were collected from six C-cells and the number of bursts in the 5 s period prior to stimulation were counted. For each cell, this number was defined as 100% prestimulus activity. The number of bursts falling into each of four 5 s bins following the stimulus were then noted and these numbers expressed as a percentage of the number of bursts in the prestimulus bin for each cell. This normalized the data for the variation of burst frequencies in different individual C-cells. The resulting histogram shows that skin stimulation reduced the frequency of C-cell bursts by about 40% in the 5 s period after the stimulus. As experiments progressed, inhibition of activity following skin stimulation was used as an adjunct to the identification of C-cells.

Physiological correlates of C-cell and C-fibre activity

In preparations where the B-fibre input was cut, the appearance of bursts of APs and/or single APs in C-cells in many, but not all C-cells correlated with the population postganglionic C-fibre discharge recorded extracellularly from the ramus communicans. Figure 10*A* illustrates simultaneous intracellular recording from a C-cell (Fig. 10*Aa*) and extracellular recording from a postganglionic nerve ramus (Fig. 10*Ab*). Each time a burst of activity occurs in the C-fibres of the ramus single APs or a burst of APs occurs in the C-cell.

Figure 10*Ba* illustrates spontaneous activity recorded extracellularly from a few preganglionic C-fibres in the VIIIth ramus communicans (point R_2 in Fig. 1*A*). The activity also comprises bursts which appear similar in frequency and duration to those recorded in C-cells (see Fig. 8) and to those recorded in the ramus communicans which emerges from the Xth ganglion (Fig. 10*Bb*).

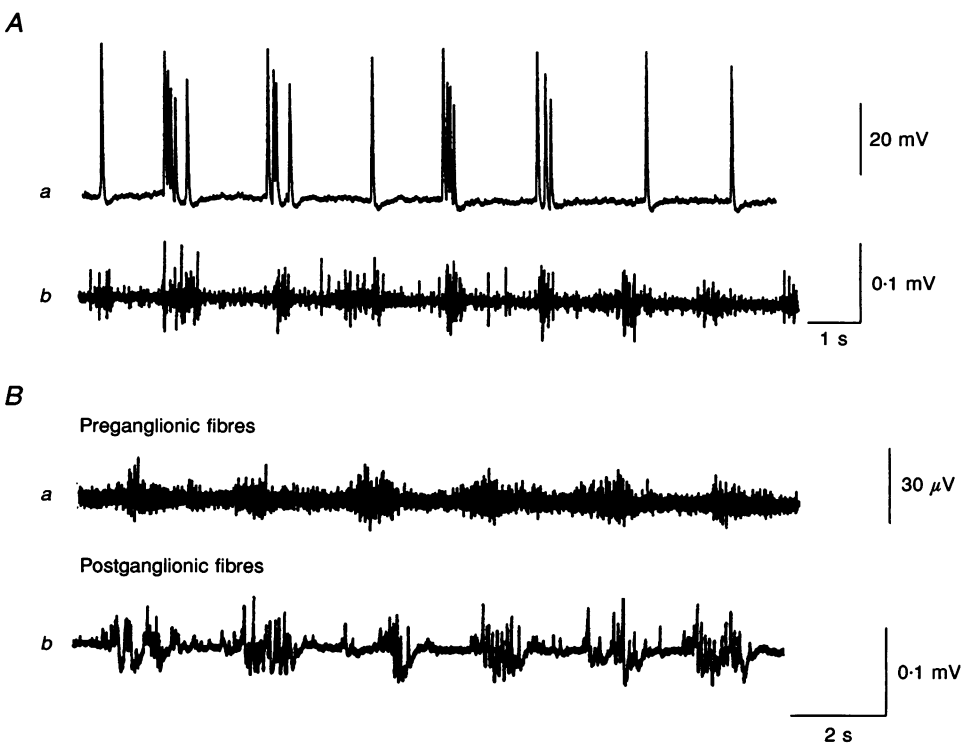

Figure 10. Comparison of intracellular activity of C-cells and pre- and postganglionic population activity

Descending B-fibre input in the paravertebral sympathetic chain had been cut to isolate C-fibre activity. Data records stored on videotape, redigitized and output on *X–Y* plotter. *A*, synchronous intracellular recording from a C-cell (*a*) and extracellular recording from the postganglionic nerve ramus (*b*). Note synchrony between population activity and intracellular activity. *B*, comparison of activity recorded from a few fibres in one of the rami of the VIIIth spinal nerve which contains the preganglionic input to C-cells and the activity in a postganglionic ramus from the Xth ganglion. Although both activities were monitored simultaneously in the same preparation, this recording configuration produced intractable noise problems. Thus, for the purpose of illustration, records *a* and *b* were acquired sequentially; preganglionic activity was recorded prior to postganglionic activity. When the first presynaptic and postsynaptic bursts are aligned, the similarity in the duration and frequency of bursts in the two sets of fibres is clearly apparent.

Activity in C-cells often correlated with cardiac activity which was measured from the ECG. The duration of the cardiac cycles ranged from 1·1 to 1·5 s. Figure 11*A a* illustrates intracellular recordings made from a C-cell at the same time as the ECG recordings illustrated in Fig. 11*A b*. The correlation is illustrated by the latency histogram (post-R cycle histogram) shown in Fig. 11*A c*. This histogram was constructed by using the large bipolar deflection (R-wave) on the ECG as the zero time point for a cardiac cycle which, in this preparation, lasted for 1·4 s. The latency between each C-cell AP and the cycle start was recorded in the appropriate 0·1 s bin. A single peak was obtained at about 1·1 s. Figure 11*B* illustrates a different situation, in which C-cell activity (Fig. 11*Ba*) was not correlated with ECG activity (Fig. 11*Bb*). This lack of correlation is apparent from the absence of a discrete peak in the post-R cycle histogram for the data which is shown in Fig. 11*Bc*.

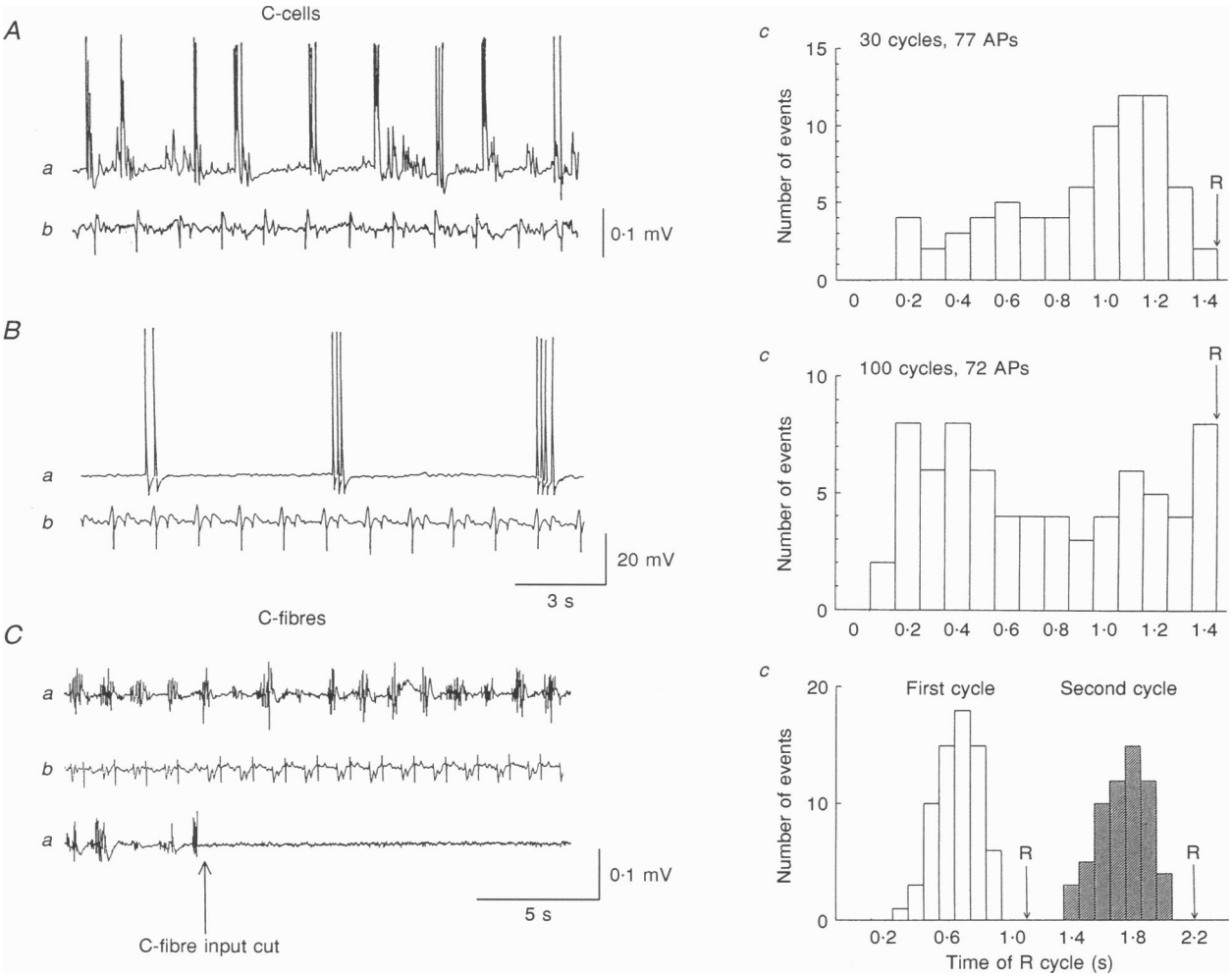

Figure 11. Comparison of C-cell or postganglionic C-fibre activity and ECG activity

In all sections of the figure, traces labelled *a* are intracellular neurone or extracellular postganglionic C-fibre recordings, traces labelled *b* are ECG recordings and traces labelled *c* are latency histograms showing the relationship between the cardiac cycle and neuronal activity. These 'post R-cycle histograms' were constructed by using the large downward deflection (R-wave) on the ECG record as time zero and measuring the latency of C-fibre APs. Latencies were grouped in 0·1 s bins. Nerve and ECG recordings were made on a rectilinear pen recorder which limits spike amplitude. *A*, intracellular recordings from a C-cell that exhibited activity which was correlated with ECG activity; the post-R cycle histogram exhibited a peak at 1·1 s. *B*, intracellular recordings from a C-cell which exhibited activity which did not correlate with ECG activity; no discrete peak is apparent in the post-R cycle histogram. *C*, extracellular recordings from postganglionic C-fibres in fine nerves which emerge from the VIIIth paravertebral ganglion and project towards the aorta (nerves marked BV in Fig. 1; B-fibre input had been cut in this preparation). The latency histogram was constructed over two cardiac cycles and two peaks are apparent at 0·7 and at 1·8 s. R designates the time of the successive R-waves. 0·1 mV calibration for ECG record (*b*) in *A* also applies to ECG records in *B* and *C*.

It is probable that those C-cells that exhibit activity which is correlated with ECG activity may function as vasomotor neurones. Although this possibility is difficult to examine directly, it is possible to record extracellularly from fine nerves which emerge from the ganglia and seem to course towards the aorta and other blood vessels (BV in Fig. 1*A*). If vasomotor C-cell activity is correlated with ECG activity, a correlation should be apparent with C-fibre activity in postganglionic vasomotor nerves. An experiment of this type is illustrated in Fig. 11*C*. Extracellular recordings were made from a small nerve which emerged from the VIIIth ganglion in a preparation where presynaptic B-fibres had been cut. Activity in the nerve ceased when the preganglionic C-fibre input was cut, indicating that all activity in the nerve originated from C-fibres (Fig. 11*Ca*). Downward deflections in the ECG record (Fig. 11*Cb*) seem to correlate with bursts of vasomotor C-fibre activity (Fig. 11*Ca*). Latencies were recorded for APs that occurred during two successive cardiac cycles which lasted for 1·1 s in this preparation. The data are shown in the histogram of Fig. 11*Cc* which shows that two peaks were obtained; one at about 0·7 s and another at 1·8 s (i.e. at 1·1 + 0·7 s). C-fibre activity was recorded from four other fine nerves which seemed to course towards blood vessels. In all cases, there appeared to be a clear correlation between nerve and ECG activity.

Peripheral projections of sympathetic nerves

Recordings were made from peripheral sympathetic nerves in three different animals to investigate the projections of vasomotor and non-vasomotor fibres. Activity was compared with ECG activity. The anatomical arrangement of these

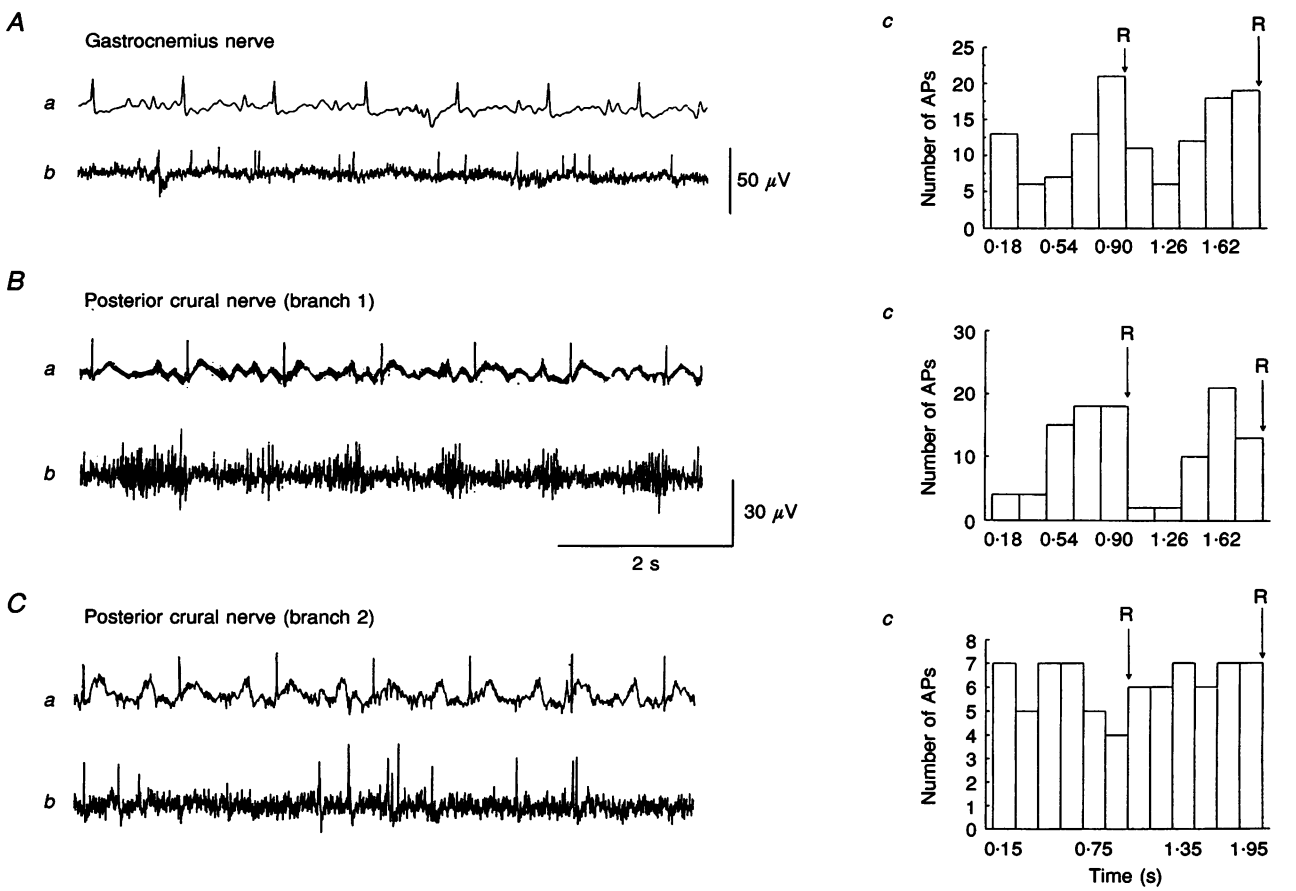

Figure 12. Comparison of peripheral sympathetic nerve activity and ECG activity

In all sections of the figure, traces labelled *a* are ECG recordings and traces labelled *b* are extracellular nerve recordings and *c* are 'post R-cycle histograms' for two cardiac cycles (see Fig. 1, legend to Fig. 11 and text for further details). R designates the time of the successive R-waves. Nerve and ECG recordings were made on a rectilinear pen recorder which attenuates the true amplitude of the extracellularly recorded population APs. *A*, recordings from gastrocnemius nerve. Note the rather broad peaks in the post-R cycle histogram *B*, recordings from one branch of the crural nerve. Note discrete peaks in the R-cycle histogram. *C*, recordings from another branch of the crural nerve. Note absence of peaks in the post R-cycle histogram. All recordings from the same preparation in which the IXth and Xth spinal nerves had been cut at their points of exit from the spinal curve. Calibration in *B* applies for both nerve and ECG recordings in sections *B* and *C*. Recordings in *A* recorded on the same time scale but at lower gain; 50 μV calibration applies to nerve and ECG recordings.

nerves is shown schematically in Fig. 1*B*. Note that the IXth and Xth spinal nerves were cut at their point of exit from the spinal cord to remove the contribution of somatic nerve activity. Figure 12*Aa* illustrates recordings made from the gastrocnemius nerve close to its point of entry to the gastrocnemius muscle and Fig 12*Bb* and *Cb* shows recordings from two different branches of the posterior crural nerve which runs along the underside of the skin of the leg. The activity in the gastrocnemius nerve (Fig. 12*A*) and in one branch of the crural nerve comprises mainly C-fibre activity. The presence of more discrete peaks in the post-R cycle histogram for the crural nerve branch (Fig. 12*Bc*) than in that for the gastrocnemius nerve (Fig. 12*Ac*) suggests that there is a better correlation between ECG activity in a cutaneous vasomotor nerve than in a muscle vasomotor nerve. Figure 12*C* illustrates recordings from another branch of the crural nerve which exhibited B-fibre activity that was not correlated with ECG activity.

Estimation of the number of B- or C-cells which discharge synchronously

Since the activity of individual B- and C-cells is correlated with population discharge of fibres in the postganglionic nerve (see Figs 5*A*, 6*B* and 10*A*) several B- or C-cells must discharge simultaneously. A similar situation obtains in rabbit superior cervical ganglion where extensive divergence and convergence of preganglionic fibres promotes synchronous discharge of 100 or more neurones (Skok & Ivanov, 1987; Ivanov & Skok, 1992). The spike-triggered averaging techniques developed by these authors were used to determine how many B- or C-cells in bullfrog paravertebral sympathetic ganglia discharge synchronously *in vivo*.

The electrical activity of postganglionic fibres emerging from the IXth ganglion via one ramus communicantes was recorded simultaneously with the intracellular potentials from a B- or a C-neurone. Spontaneous intracellular APs

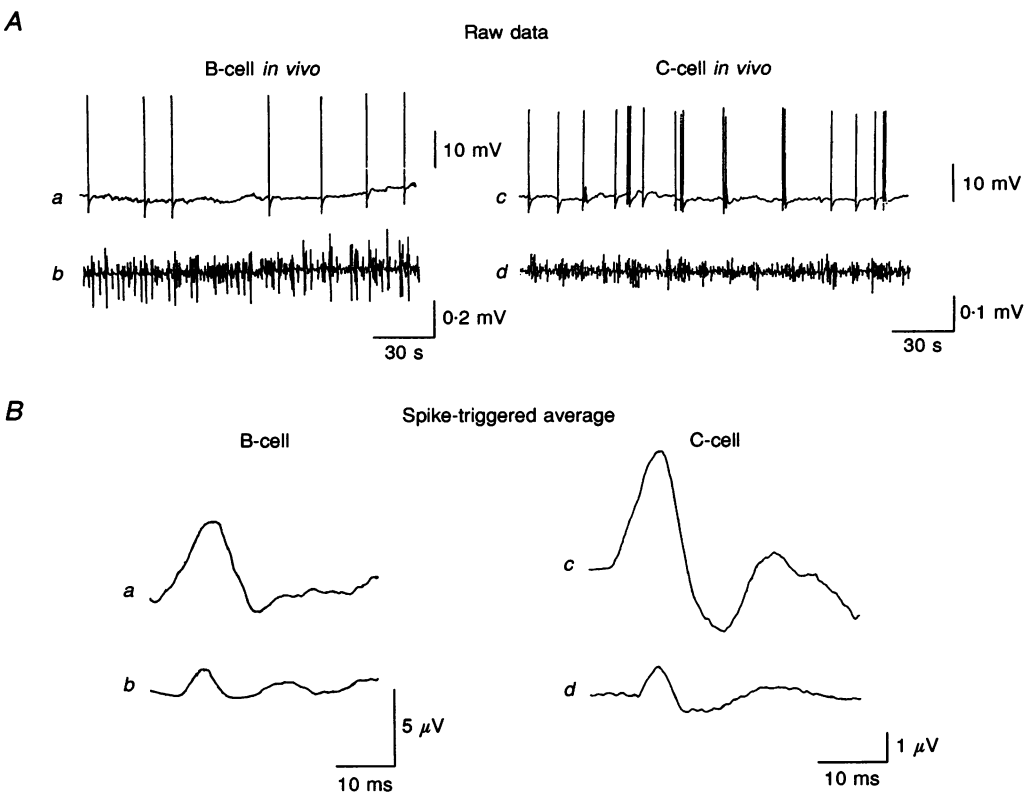

Figure 13. Spike-triggered averaging experiment to determine the number of B- and C-cells which discharge spontaneously *in vivo*

Aa, intracellular recording from a B-cell; *Ab*, extracellular recording from postganglionic ramus communicans; *Ac*, intracellular recording from a C-cell; *Ad*, extracellular recording from postganglionic ramus communicans. B- and C-cell data obtained from different preparations and recorded on a rectilinear pen recorder which attenuates spike amplitude because of its limited frequency response. *B*, spike-triggered average data obtained from extracellular recordings obtained in *Ab* and *Ad*. *Ba*, B-cell data triggered from spontaneous APs; *Bb*, B-cell data triggered by intracellular stimulation of the cell illustrated in *Aa*; *Bc*, C-cell data triggered from spontaneous APs; *Bd*, C-cell data triggered by intracellular stimulation of the cell illustrated in *Ac*. Records in *B* are *X*–*Y* plots of signals averaged on a digital oscilloscope.

triggered the storing and averaging of 55 ms of postganglionic nerve activity on a digital oscilloscope. After storing spontaneous activity, the same cell was stimulated directly through the microelectrode by using 20 ms depolarizing pulses and the resulting intracellular AP used to trigger the averaging of 55 ms of activity recorded from postganglionic fibres. (Usually from 25 to 100 sweeps were stored and averaged.) The number of neurones discharging synchronously with the identified cell is determined by the ratio of the areas of the former signal to the later signal (Skok & Ivanov, 1987; Ivanov & Skok, 1992).

Eight B-cells and six C-cells were investigated in this way. Typical experiments on a B- and C-cell are illustrated in Fig. 13. The intracellular and extracellular recordings of spontaneous activity are illustrated in the upper traces (Fig. 13*A*). Averaged responses recorded from the postganglionic nerve, which were triggered by spontaneous, intracellular APs, are shown in Fig. 13*Ba* and *c*. The data from the C-cell (Fig. 13*Bc*) exhibits two clear peaks, the second of which may have reflected the tendency for C-cells to exhibit bursting behaviour. The lower records (Fig. 13*B c* and *d*) illustrate the averaged signals from the postganglionic nerve which were triggered by evoked APs in the cell bodies. For B-cells, the area of the signal stored when averaging was triggered by spontaneous intracellular APs ranged from 37 to 124 μV ms (mean value was 81·5 $\pm$ 12·5 μV ms, $n = 8$). The area of signals produced when averaging was triggered by APs evoked in the recorded neurone using direct stimulation was much smaller and ranged from 1·2 to 5·6 μV ms (mean 3·4 $\pm$ 0·5 μV ms, $n = 8$). Division of the corresponding areas for each individual cell showed that thirteen to thirty-six (average 23) B-cells discharge synchronously in the 9th ganglion *in vivo*. Similar calculations applied to the C-cell data showed that thirteen to twenty-eight (average 21) cells discharge synchronously.

If a given preganglionic fibre activates neurones which project through different rami, this method would provide an underestimate of the number of cells innervated.

DISCUSSION

Whilst it is difficult to know how the activity of sympathetic nerves in anaesthetized frogs relates to their activity in conscious animals, *in vivo* experiments on urethane-treated frogs represent the only feasible approach by which to study the activity of autonomic nerves and their associated ganglia. Despite that constraint, the results presented in this paper still reveal several interesting aspects of the amphibian sympathetic system which are not available from *in vitro* experiments. For example, identified B-cells, which primarily innervate glands in the skin, have a very different pattern of activity from C-cells, which primarily, but not exclusively, innervate blood vessels. Differences are apparent in different groups of C-cells which may innervate different targets.

Since about twenty-one C-cells and about twenty-three B-cells discharge synchronously in response to each preganglionic AP and this is very close to the size of a neuronal unit calculated from the ratio of the number of preganglionic fibres to the number of B- or C-cells in BFSG (Horn & Stofer, 1988), the synchrony of discharge is likely to result from the divergence of preganglionic axons. Convergence does not play as important a role as it does in mammalian sympathetic ganglia (Skok & Ivanov, 1987; Ivanov & Skok, 1992).

Characteristics of B-sympathetic pathways

Electrophysiological and morphological data support the idea that each B-cell is innervated by a single presynaptic B-fibre which descends in the ipsilateral paravertebral sympathetic chain (Nishi *et al.* 1965; Weitsen & Weight, 1977; Baluk, 1986). Activation of these fibres *in vitro* produces a large, all-or-none EPSP which almost invariably exceeds threshold for AP generation (Smith, 1994). Since the majority of the APs recorded *in vivo* had a very sharp rising phase, it is likely that they were generated from a large EPSP that resulted from a single preganglionic fibre in the ipsilateral sympathetic chain. Had summation of inputs from several presynaptic fibres been required, some inflexions would have been present in the rising phase of the AP (see Skok & Ivanoff, 1983). The observation that 59 out of 126 of the identified B-cells studied *in vivo* did exhibit both APs and subthreshold EPSPs was therefore quite unexpected. Because B-cells which exhibited only subthreshold EPSPs and B-cells which exhibited sharp, spontaneous APS were encountered in every animal examined, it is unlikely that appearance of subthreshold responses is an artifact of urethane anaesthesia. Two possible explanations for the presence of subthreshold EPSPs remain feasible: either (i) EPSPs generated by a single presynaptic B-fibre are subject to strong inhibitory presynaptic modulation *in vivo* which is not present *in vitro* or (ii) B-cells receive additional weak excitatory inputs through fibres which are not activated under the usual conditions of *in vitro* experiments. One possible source of such fibres is the fine nerves which run laterally from the paravertebral sympathetic chain. The result that complete elimination of B-fibre activity in Xth nerve rami requires interruption of both the ipsilateral sympathetic chain and the fine lateral sympathetic nerves is consistent with this possibility (see Fig. 3). It might therefore be suggested that 59 out of the 120 B-cells which exhibited spontaneous activity receive a 'dominant' suprathreshold input from the ipsilateral sympathetic chain and weaker subthreshold inputs from the contralateral chain (see Skok & Ivanoff, 1987). The weaker input may occasionally be strong enough to evoke an AP and this may account for the presence of EPSPs with different rates of rise leading to inflexions in the upshoot of the AP in four of the B-cells studied. We therefore estimate that 63 of 120 (53%) B-cells receive convergence of input whereas the remainder receive input from a single B-fibre, as was originally suggested from the *in vitro* data (Nishi &

Koketsu, 1960; Nishi *et al.* 1965; Weitsen & Weight, 1977; Smith & Weight, 1986; Baluk, 1986).

It is possible that synchronous activation of convergent fibres during activation of reflex responses could generate an AP as a result of temporal summation of a few EPSPs. However, no such summation was observed when reflex discharge was evoked in B-cells following tactile or nociceptive stimulation of the skin. Thus, the subthreshold EPSPs may have another functional role; perhaps they generate APs during the development of the peptidergic late–slow EPSP in B-cells as has been demonstrated *in vitro* (Schulman & Weight, 1976).

The list of probable targets in the skin that can be innervated by B-cells includes mucous and granular glands (Honma, 1970), cold receptors (Spray, 1974) and mechanoreceptors (Loewenstein, 1956; Lang *et al.* 1975). Although these targets receive a low-frequency sympathetic discharge without any baroreceptor modulation (about 40% of B-cells had a frequency of APs lower than 0·1 s^{-1}), these low-discharge frequencies are unlikely to result from selective depression of sympathetic transmission to B-cells as a result of urethane anaesthesia because the frequency of APs ranged widely in different cells in the same animal (from 0·01 to 0·4 s^{-1}). The difference in the frequency of sympathetic discharge found in different B-cells is probably related to the targets they innervate. Both 'fast' and 'slow' B-cells must innervate targets in the skin because their axons are found in all cutaneous nerves (Horn *et al.* 1988). Furthermore, both types of B-cells showed the same kind of excitatory responses when tactile or nociceptive receptors were stimulated. The only difference in their patterns of activity was that 'slow' B-cells exhibited a slightly higher frequency of discharge and less subthreshold activity than 'fast' B-cells. It is interesting in this regard that the pattern of activity and frequency of discharge in B-cells is similar to that of those rat superior cervical ganglion (SCG) cells which innervate the submandibular gland (Ivanov, 1991). Because cells which innervate the submandibular gland in the rat are the largest cells in SCG (Leubke & Wright, 1992) and B-cells are the larger of the two cell types in BFSG (Dodd & Horn 1983*a*), it may be that larger ganglion cells generally exhibit a low-frequency of spontaneous activity and project to exocrine glands.

Characteristics of C-sympathetic pathways

In vitro and *in vivo* experiments have shown that the stimulation of preganglionic C-fibres produces cutaneous and muscular vasoconstriction in the toad (Honma, 1970) and bullfrog (Yoshimura, 1979; Stofer *et al.* 1990). These data suggest that C-cells are involved in vasomotor sympathetic pathways. It is important to characterize C-fibre activity in order to understand how the sympathetic system regulates the function of the circulatory system (see Horn, 1992). The present data show that a burst pattern of discharge is found in the C-cells of BFSG. The bursts occur with a frequency of 0·3–0·7 s^{-1} and every burst consists of three to six APs. Thus, the total number of APs per unit time spreading to blood vessels is considerably higher than the number of APs spreading through B-cells to effector organs.

Since bursts of electrical activity could be recorded from both postganglionic and preganglionic fibres, the burst of APs recorded intracellularly in each C-cell probably results from a burst of APs in a preganglionic neurone in the spinal cord. This conclusion is supported by the observation that bursts of subthreshold EPSPs occurred in C-cells at similar frequencies to bursts of APs (see Fig. 8*C*). Under certain conditions, however, C-cells can generate busting activity as a result of their intrinsic biophysical properties and as a result of interactions between the muscarinic slow IPSP and the peptidergic late–slow EPSP (Horn & Dodd, 1983*b*; Horn 1992). It remains to be determined whether these mechanisms contribute to the fine structure of the bursts seen in C-cells *in vivo*.

Intracellular recordings from 67% of the C-cells studied and/or recordings from postganglionic C-fibres showed good correlation with the cardiac cycle, indicating that activity in many cells is susceptible to baroreceptor influence. Those C-cells which did not exhibit activity which was correlated with the ECG may have projected to non-vascular targets such as the bladder (Horn *et al.* 1988). In mammals, the activity of neurones that innervate blood vessels in skeletal muscle is modulated by baroreceptor input whereas the activity in neurones that innervate blood vessels in the skin is not (Ivanoff, 1987; Janig, 1988). In the bullfrog, however, our data show that activity recorded from C-fibres in both muscle sympathetic nerves and from some cutaneous sympathetic nerves is synchronized with the cardiac cycle (see Fig. 12). Moreover, the synchronization was better expressed in a cutaneous nerve compared with a muscle nerve.

Interactions between the B- and C-sympathetic pathways and physiological relevance of slow synaptic potentials

The increase in activity of B-cells and inhibition of activity of C-cells following tactile or nociceptive stimulation of the skin may reflect an interaction of the B- and C-fibre systems within the central nervous system. Because stimulation of C-fibres at 'physiological' frequencies increases the spontaneous firing rate of B-cells (Fig. 5*C*) and evokes a discharge in B-fibres (Fig. 7), an additional interaction between the two systems occurs at the level of the ganglion. This perhaps reflects neurotransmitter action 'at a distance' and the modulatory influence of the C-fibre late–slow EPSP on B-cell activity (Jan *et al.* 1979, 1980). Activation of this mechanism does not appear to alter the membrane properties of B-cells such that they generate spontaneous APs (Dodd & Horn 1983*b*) but may instead increase the amplitude of spontaneous subthreshold EPSPs such that they approach the threshold for AP generation (see Schulman & Weight, 1976). This conclusion is reinforced by the observation that C-fibre stimulation fails to evoke

B-fibre activity in the postganglionic nerve rami of preparations where the preganglionic B-fibre input has been cut (i.e. in preparations where there is no spontaneous synaptic activity in B-cells; A. Y. Ivanoff and P. A. Smith, unpublished observations).

There are some questions relating to the exact mechanism of generation of the B-fibre after-discharge. Whilst it has been argued that the response results from the transition of subthreshold EPSPs to suprathreshold levels, the effects seen with intracellular recording in B-cells are significant but quite small (Fig. 5*C*). Another concern is that subthreshold activity in B-cells appears to originate from the contralateral sympathetic chain and that activity from the ipsilateral chain is normally suprathreshold. If this is the case, it is difficult to explain why after-discharge is prevented by cutting ipsilateral B-fibres because this would remove suprathreshold activity rather than subthreshold activity which may be susceptible to modulation via the late–slow EPSP mechanism.

One of the most widespread objections to the possible role of slow synaptic potentials in the physiological modulation of ganglionic transmission is that the intense stimulation used to evoke the slow IPSP, slow EPSP and late–slow EPSP *in vitro* is far higher than the level of activity that has been assumed to occur *in vivo* (Ginsborg, 1976). Although no obvious, discrete, spontaneous slow IPSP were observed during *in vivo* recording from C-cells, this observation does not preclude a role for inhibitory muscarinic effects. Although slow IPSPs can be recorded *in vitro* in response to a single preganglionic stimulus (Smith & Weight, 1986; Smith, 1994) and the burst pattern of activity observed in C-cells might be expected to induce a large slow IPSP (Horn & Dodd, 1983*b*), additional experiments with the blockers of muscarinic receptors must be done to establish any functional role for the slow IPSP *in vivo*. Data shown in Fig. 7 are, however, consistent with the possibility that the late–slow EPSP mechanism is invoked *in vivo* in B-cells as a result of physiological impulse traffic in preganglionic C-fibres. By contrast, the present experiments provide little evidence for a physiological role for the muscarinic slow EPSP in the modulation of activity of BFSG. The spontaneous slow depolarizations illustrated in Fig. 5*A* were obtained in a preparation where the C-fibres were intact and may therefore have represented the late–slow EPSP mechanism rather than the slow EPSP mechanism. Furthermore, reflex activation of B-cells following skin stimulation only rarely evoked slow depolarizations in B-cells. In some experiments, however, excitability was enhanced for prolonged periods following skin stimulation (see Fig. 6*B*) and this could reflect prolonged muscarinic suppression of M-current which would not necessarily promote membrane depolarization (Jones, 1985) yet would promote prolonged periods of increased excitability. However, the observation that the enduring discharge was correlated with the population response of the postganglionic axon suggests that a central rather than a peripheral mechanism may be involved. Taken together, these observations suggest that under the conditions of our experiments (i.e. in urethane-anaesthetized frogs), that the peptidergic late–slow EPSP is much more likely to play a role in ganglionic transmission *in vivo* than the muscarinic slow EPSP.

Adams, P. R., Jones, S. W., Pennefather, P. S., Brown, D. A., Koch, C. & Lancaster, B. (1986). Slow synaptic transmission in frog sympathetic ganglia. *Journal of Experimental Biology* **124**, 259–285.

Baluk, P. (1986). Scanning electron microscopic studies of bullfrog sympathetic neurons exposed by enzymatic removal of connective tissue elements and satellite cells. *Journal of Neurocytology* **15**, 85–95.

Dodd, J. & Horn, J. P. (1983*a*). A reclassification of B and C neurons in the ninth and tenth paravertebral sympathetic ganglion of the bullfrog. *Journal of Physiology* **334**, 255–269.

Dodd, J. & Horn, J. P. (1983*b*). Muscarinic inhibition of sympathetic C-cells in the bullfrog. *Journal of Physiology* **334**, 271–291.

Ginsborg, B. L. (1976). *Physiology of the Autonomic Nervous System in Frog Neurobiology: A Handbook*, ed. Llinas, R. & Precht, W., pp. 151–168. Springer Verlag, Berlin.

Honma, S. (1970). Functional differentiation in sB and sC neurons of toad sympathetic ganglia. *Japanese Journal of Physiology* **20**, 281–295.

Horn, J. P. (1992). The integrative role of synaptic co-transmission in the bullfrog vasomotor C system: evidence for a synaptic gain hypothesis. *Canadian Journal of Physiology and Pharmacology*, suppl., **70**, S19–26.

Horn, J. P. & Dodd, J. (1981). Monosynaptic muscarinic activation of K^+ conductance underlies the slow inhibitory postsynaptic potential in sympathetic ganglia. *Nature* **292**, 625–627.

Horn, J. P., Fatherazi, S. & Stofer, W. D. (1988). Differential projections of B and C sympathetic axons in peripheral nerves of the bullfrog. *Journal of Comparative Neurology* **278**, 570–580.

Horn, J. P. & Stofer, W. D. (1988). Spinal origins of preganglionic B and C neurons that innervate paravertebral sympathetic ganglia nine and ten of the bullfrog. *Journal of Comparative Neurology* **268**, 71–83.

Ivanoff, A. Y. (1987). Patterns of tonic activity in different groups of rabbit superior cervical ganglion neurones. *Neurophysiologica* **19**, 495–501.

Ivanoff, A. Y. (1991). Pattern of ongoing activity in rat superior cervical ganglion neurons projecting to a specific target. *Journal of the Autonomic Nervous System* **32**, 77–80.

Ivanoff, A. Y. & Skok, V. I. (1992). Neuronal mechanisms responsible for ongoing activity of rabbit superior cervical ganglion neurons. *Journal of the Autonomic Nervous System* **41**, 61–66.

Ivanoff, A. Y. & Smith, P. A. (1993). Activity of bullfrog sympathetic neurones *in vivo*. *Society for Neuroscience Abstracts* **19**, 1524.

Jan, Y. N., Jan, L. Y. & Kuffler, S. W. (1979). A peptide as a possible transmitter in sympathetic ganglia of the frog. *Proceedings of the National Academy of Sciences of the USA* **76**, 1501–1505.

Jan, Y. N., Jan, L. Y. & Kuffler, S. W. (1980). Further evidence for peptidergic transmission in sympathetic ganglia. *Proceedings of the National Academy of Sciences of the USA* **77**, 5008–5012.

Janig, W. (1988). Pre- and postganglionic vasoconstrictor neurons: differentiation, types and discharge properties. *Annual Review of Physiology* **50**, 525–539.

JANIG, W. & MCLACHLAN, E. M. (1992). Characteristics of function specific pathways in the sympathetic nervous system. *Trends in Neurosciences* **15**, 476–481.

JONES, S. W. (1985). Muscarinic and peptidergic excitation of bull-frog sympathetic neurones. *Journal of Physiology* **366**, 63–87.

JONES, S. W., ADAMS, P. R., BROWNSTEIN, M. J. & RIVIER, J. E. (1984). Teleost luteinizing hormone releasing hormone: action on bullfrog sympathetic ganglia is consistent with role as neurotransmitter. *Journal of Neuroscience* **4**, 420–429.

KUBA, K. & KOKETSU, K. (1978). Synaptic events in sympathetic ganglia. *Progress in Neurobiology* **11**, 77–169.

LANG, L., SJOBERG, E. & SKOGLUND, C. R. (1975). Conductance recording of ionic outflow from frog skin glands during nerve stimulation. *Acta Physiologica Scandinavica* **93**, 67–76.

LEUBKE, J. I. & WRIGHT, L. L. (1992). Characterization of superior cervical ganglion neurons that project to the submandibular glands, the eyes, and the pineal glands. *Brain Research* **589**, 1–14.

LIBET, B., CHICHIBU, S. & TOSAKA, T. (1968). Slow synaptic responses and excitability in sympathetic ganglia of the bullfrog. *Journal of Neurophysiology* **31**, 383–395.

LOEWENSTEIN, W. R. (1956). Modulation of cutaneous mechanoreceptors by sympathetic stimulation. *Journal of Physiology* **132**, 40–60.

NISHI, S. & KOKETSU, K. (1960). Electrical properties and activities of single sympathetic neurons in frogs. *Journal of Cellular and Comparative Physiology* **55**, 15–30.

NISHI, S., SOEDA, H. & KOKETSU, K. (1965). Studies on sympathetic B and C neurons and patterns of preganglionic innervation. *Journal of Cellular and Comparative Physiology* **66**, 19–32.

SCHULMAN, J. A. & WEIGHT, F. F. (1976). Synaptic transmission: Long-lasting potentiation by a postsynaptic mechanism. *Science* **194**, 1437–1439.

SKOK, V. I. (1973). *Physiology of Autonomic Ganglia*. Igaku Shoin, Tokyo.

SKOK, V. I. & IVANOFF, A. Y. (1987). Organization of presynaptic inputs to neurones of a sympathetic ganglion. In *Organization of the Autonomic Nervous System: Central and Peripheral Mechanisms*, ed. CIRIELLO, J., CALARESU, F. R., RENAUD, L. P. & POLOSA, C., pp. 37–46. Alan R. Liss, New York.

SMITH, P. A. (1994). Amphibian sympathetic ganglia: an owner's and operator's manual. *Progress in Neurobiology* **43**, 439–510.

SMITH, P. A. & WEIGHT, F. F. (1986). The synaptic pathway for the slow inhibitory postsynaptic potential in amphibian sympathetic ganglia. *Journal of Neurophysiology* **56**, 823–834.

SPRAY, D. C. (1974). Characteristics, specificity and efferent control of frog cutaneous cold receptors. *Journal of Physiology* **237**, 15–38.

STOFER, W. D., FATHERAZI, S. & HORN, J. P. (1990). Neuropeptide Y mimics a non-adrenergic component of sympathetic vasoconstriction in the bullfrog. *Journal of the Autonomic Nervous System* **31**, 141–152.

TOSAKA, T., CHICHIBU, S. & LIBET, B. (1968). Intracellular analysis of slow inhibitory and excitatory postsynaptic potentials in sympathetic ganglia of the frog. *Journal of Neurophysiology* **31**, 396–409.

WEIGHT, F. F. & PADJEN, A. (1973*a*). Slow synaptic inhibition: evidence for synaptic inactivation of sodium conductance in sympathetic ganglion cells. *Brain Research* **55**, 214–219.

WEIGHT, F. F. & PADJEN, A. (1973*b*). Acetylcholine and slow synaptic inhibition in frog sympathetic ganglion cells. *Brain Research* **55**, 225–228.

WEIGHT, F. F. & VOTAVA, J. (1970). Slow synaptic excitation in sympathetic ganglion cells: evidence for synaptic inactivation of potassium conductance. *Science* **170**, 755–758.

WEITSEN, H. A. & WEIGHT, F. F. (1977). Synaptic innervation of sympathetic ganglion cells in bullfrog. *Brain Research* **128**, 197–211.

YOSHIMURA, M. (1979). Tonic and reflex discharges of sympathetic ganglion cells. *Journal of the Kurume Medical Association* **42**, 1221–1238.

Acknowledgements

This work was supported by the Medical Research Council of Canada. We thank Dr John P. Horn for his comments on an early version of this manuscript and Tina Cho for preparing the diagram shown in Fig. 1.

Author's present address

A. Y. Ivanoff: Bogomoletz Institute of Physiology, Kiev 24, Ukraine.

Received 28 January 1994; accepted 2 December 1994.